



OPEN ACCESS

EDITED BY

Bernd Grambow,
UMR6457 Laboratoire de Physique
Subatomique et des Technologies Associées
(SUBATECH), France

REVIEWED BY

Sayandev Chatterjee,
TerraPower LLC, United States
Olaf Kolditz,
Helmholtz Centre for Environmental Research,
Germany

*CORRESPONDENCE

María Victoria Villar,
✉ mv.villar@ciemat.es
Christophe de Lesquen,
✉ christophe.delesquen@andra.fr
Arnaud Dizier,
✉ arnaud.dizier@euridice.be
Dragan Grgic,
✉ dragan.grgic@univ-lorraine.fr

RECEIVED 22 May 2024

ACCEPTED 20 February 2025

PUBLISHED 28 March 2025

CITATION

Villar MV, Bésuelle P, Collin F, Cuss R,
de Lesquen C, Dizier A, El Tabbal G, Gens A,
Graham C, Grgic D, Harrington J, Imbert C,
Leupin O, Levasseur S, Narkūnienė A, Simo E
and Tatomir A-B (2025) EURAD state-of-the-art
report: thermo-hydro-mechanical behaviour at
high temperature of host clay formations.
Front. Nucl. Eng. 4:1436490.
doi: 10.3389/fnuen.2025.1436490

COPYRIGHT

© 2025 Villar, Bésuelle, Collin, Cuss, de
Lesquen, Dizier, El Tabbal, Gens, Graham, Grgic,
Harrington, Imbert, Leupin, Levasseur,
Narkūnienė, Simo and Tatomir. This is an open-
access article distributed under the terms of the
[Creative Commons Attribution License \(CC BY\)](https://creativecommons.org/licenses/by/4.0/).
The use, distribution or reproduction in other
forums is permitted, provided the original
author(s) and the copyright owner(s) are
credited and that the original publication in this
journal is cited, in accordance with accepted
academic practice. No use, distribution or
reproduction is permitted which does not
comply with these terms.

EURAD state-of-the-art report: thermo-hydro-mechanical behaviour at high temperature of host clay formations

María Victoria Villar^{1*}, Pierre Bésuelle², Frédéric Collin³,
Robert Cuss⁴, Christophe de Lesquen^{5*}, Arnaud Dizier^{6*},
Ginger El Tabbal⁷, Antonio Gens⁸, Caroline Graham⁴,
Dragan Grgic^{9*}, Jon Harrington⁴, Christophe Imbert¹⁰,
Olivier Leupin¹¹, Séverine Levasseur¹², Asta Narkūnienė¹³,
Eric Simo¹⁴ and Alexandru-Bogdan Tatomir¹⁴

¹Centro de Investigaciones Energéticas, Medioambientales y Tecnológicas (CIEMAT), Madrid, Spain, ²Université Grenoble Alpes (UGA) & CNRS, Grenoble, France, ³Université de Liège (ULiège), Liege, Belgium, ⁴British Geological Survey (BGS), Nottingham, United Kingdom, ⁵Agence Nationale pour la Gestion des Déchets Radioactifs (ANDRA), Châtenay-Malabry, France, ⁶European Underground Research Infrastructure for Disposal of nuclear waste in a Clay Environment (EURIDICE), Mol, Belgium, ⁷Electricité de France (EDF), Paris, France, ⁸Universitat Politècnica de Catalunya (UPC), Barcelona, Spain, ⁹Université de Lorraine (ULorraine), Nancy, France, ¹⁰Commissariat à l'Energie Atomique (CEA), Paris, France, ¹¹Nationale Genossenschaft für die Lagerung radioaktiver Abfälle (NAGRA), Wetztingen, Switzerland, ¹²Belgian agency for radioactive waste and enriched fissile materials (ONDRAF/NIRAS), Brussels, Belgium, ¹³Lithuanian Energy Institute (LEI), Kaunas, Lithuania, ¹⁴Bundesgesellschaft für Endlagerung (BGE), Peine, Germany

Most safety cases for radioactive waste disposal concepts consider a temperature limit of 90°C in the clay host rock. Being able to tolerate higher temperature would have significant advantages. For this reason, part of the EURAD-HITEC project aimed at determining the influence of temperature above 90°C on clay host rock properties, trying to establish the possible extent of elevated temperature damage in the near and far field of clay host rock formations and the consequences of any such damage. Three clay formations considered to host radioactive waste repositories in Europe were the focus of the studies: the Boom Clay, the Callovo-Oxfordian claystone and the Opalinus Clay. A summary of the background knowledge about the thermo-hydro-mechanical behaviour of these clay host rocks is first presented. Then, the experimental and modelling activities carried out in the framework of the EURAD-HITEC project concerning these materials have been synthesised. The laboratory tests analysed the impact of temperature on the short- and long-term behaviour of the clay host rock and the self-sealing processes. Hydro-mechanical couplings between peak pore water pressure, temperature, permeability and confining stress were identified. The results confirmed that the claystone keeps its good mechanical and retention properties even when heated up to 100°C. Provided that the clay content of the samples is high enough, self-sealing was an efficient mechanism whatever the experimental conditions, although temperature may have a delaying effect. Poro-elastic models were used to model generic cases of a high-level waste repository, and consistent results were obtained by the different codes and teams, which shows the robustness of the modelling approach used to design the repositories. Two heating tests, performed in the HADES (Belgium) and MHM (France) underground research laboratories, were selected as benchmarks for the

modelling activities. The evolutions of temperature and pore pressure were well modelled in the far field with a poro-elastic approach, but more advanced models are needed to take into account the processes occurring around the tunnels (e.g., modification of hydraulic properties within the EDZ, creep). The modelling of laboratory experiments showed the importance of a good understanding of the tests setup and of the boundary conditions.

KEYWORDS

claystone, radioactive waste, thermo-hydraulic behaviour, creep, hydraulic conductivity, temperature, numerical modelling, anisotropy

1 Introduction

The work package “Influence of Temperature on Clay-based Material Behaviour” (WP7) of the EURAD Project aimed to develop and document improved thermo-hydro-mechanical (THM) understanding of clay-based materials (host rocks and buffers) exposed at high temperatures or having experienced high temperature transients for extended durations. The WP’s *raison d’être* was to evaluate whether or not elevated temperature limits (up to 150°C for the clay buffer and ~90°C for the host rock) are feasible for a variety of geological disposal concepts for high heat generating wastes (high-level waste, HLW). For the disposal of HLW it is important to understand the consequences of the heat produced on the properties and long-term performance of the natural and engineered clay barriers. Being able to tolerate higher temperature, whilst still ensuring an appropriate performance, would have significant advantages (e.g., shorter above-ground cooling times, more efficient packaging, fewer disposal containers, fewer transport operations, smaller facility footprints, etc.). Consequently, HITEC is a step toward optimization of the architecture of the deep geological disposal, since the range of temperatures tested had not been considered systematically in previous research.

HITEC studied the possible extent of elevated temperature damage in the near and far field of clay host rock formations (e.g., from over-pressurisation) and indicated the likely consequences of any such damage. Drilling underground galleries or boreholes leads to stress redistribution around the hole and some damage in the near field. Fractures are likely to form around the repository as it is constructed. The stress that was supported by the material removed during construction must be taken up by the remaining rock, leading to stress concentrations. Depending on the strength of the host-rock, this stress concentration is likely to result in fracturing and the formation of an excavation damaged zone (EDZ). The EDZ has different mechanical, hydraulic and thermal properties to the sound host rock, and the thermal impact on it can also be different. This is why an important part of the experimental activities in HITEC was devoted to the temperature influence on self-sealing.

The WP also looked at bentonite buffers and determined the temperature influence on buffer properties, trying to establish if the buffer safety functions are unacceptably impaired. These activities are described in a companion paper, where the common features of geological waste disposal concepts of the participant organisations are also summarised, for a better contextualisation of the research performed.

Previous related research activities were performed in the TIMODAZ project, that analysed the evolution of the EDZ

during the thermal transient in the context of a geological repository for heat-emitting waste in plastic and indurated clay host rocks (Yu et al., 2010). The project focused on the possible additional damage created by the thermal load. The knowledge gathered during the project indicated that an increase in temperature due to the presence of heat-emitting wastes will induce strong and anisotropic thermo-hydro-mechanical (THM) coupled responses within the clay. The thermal expansion of pore water and the thermal-induced decrease of clay strength may pose a risk of additional mechanical damage. However, no evidence was found throughout the TIMODAZ experimental programme showing temperature-induced additional opening of fractures or a significant permeability increase of the EDZ. The project also concluded that, with the current knowledge, the capacity of the repository host rock to perform its intended role as a barrier and to maintain the long-term safety functions of the system will still be preserved, in spite of the combined effect of the inevitable EDZ and the thermal output from the waste (Yu et al., 2010). It was concluded that the properties of the clay host rock that guarantee the effectiveness of the safety functions of the repository system would be maintained after the heating-cooling cycle, but this has to be confirmed with the techniques developed in the last decade and the results of new large-scale *in situ* tests also for the far field.

In the following sections syntheses of the state of knowledge on the THM behaviour at different temperatures of clay formations considered as potential host rocks in different countries (namely, Boom Clay, Callovo-Oxfordian claystone and Opalinus clay) are presented, along with the progress made during HITEC. The characteristics of the clay host rocks analysed during the project are described and their thermal, hydraulic and mechanical properties are summarised. Experimental procedures, processes, parameters and models available for low or high temperature as well as those developed during the project for the various host rocks are summarised. A significant effort has been devoted to the development of state-of-the-art equipment. Large-scale *in situ* experiments carried out in Underground Research Laboratories (URL) and modelled during the project are briefly described.

2 Properties of clay host rocks and temperature impact on them

The following subsections aim at summarising the relevant properties of the three claystone formations proposed to host radioactive waste and analysed during HITEC:

- The Boom Clay Formation. A marine deposit from the Oligocene (Rupelian stage), between 33.9 and 28.4 Ma. The formation is composed of rhythmically alternating clay-rich and silt-rich materials resulting in a grey-tone banding. The Boom Clay is a poorly indurated clay with a well-developed particle alignment according to the bedding plane and high porosity (Vandenberghé et al., 2014).
- The Callovo-Oxfordian (Cox) claystone. Deposited 160 Ma ago (Middle-Upper Jurassic) over a period of approximately 5 Ma, in an open and calm marine environment. It consists of three major geological units, the relevant one being the argillaceous unit (UA) at the base, the most homogeneous and the richest in argillaceous minerals (more than 40% on average) of the three (e.g., Rebours et al., 2005).
- Opalinus Clay (OPA). It occurs extensively in northern Switzerland and neighbouring countries. It is a moderately over-consolidated claystone originated from shallow marine sedimentation in the Middle Jurassic period (Aleanian), ~173 Ma ago, with a complex burial and compaction history. It shows a low variability in facies and lithology, with a clay mineral content >40 wt% (e.g., NAGRA, 2014).

Hence, all of them were deposited in a marine environment. As a consequence of their geologic histories (burial, subsidence, uplift, erosion) and particular mineralogy and grain size, the resulting porosity and mechanical characteristics are considerably different. Thus, the Boom Clay, which is the youngest and subjected to less burial, has a porosity of 35%–40%, consequently with higher hydraulic conductivity and lower thermal conductivity than the other clays. It can be considered as a poorly indurated clay (overconsolidation ratio, OCR = 2.4 at the level of the URL) (Horseman et al., 1987; Bernier et al., 2007a; Li et al., 2023). In contrast, the Cox claystone has a porosity of 14%–20% and the Opalinus clay of 10%–16%, having been subjected to large extent of diagenesis and tectonic activity (in the case of Opalinus). The two are much stiffer than the Boom Clay, they can be considered as moderately over-consolidated claystones and are brittle materials at low confining pressure and more ductile at high confining pressure.

Supplementary Tables summarise the mineralogical and pore water composition, hydraulic, thermal and mechanical properties of the three clays supported by appropriate references. The following sections summarise aspects of the geology of the formations, general parameters and, in different subsections, the hydro-mechanical and THM properties derived from laboratory tests and the impact of temperature on some of them. In particular, the following temperature-dependent material properties are considered to be important (Li et al., 2023): hydraulic conductivity, thermal conductivity, stiffness and strength, creep rates and the thermal sensibility on anisotropy. Information on the mechanical, hydraulic and thermal properties of the EDZ is also given below, because these properties may be different to those of the sound host rock. Most of the information gathered comes from research projects (including thesis) financed by or with participation of the waste management organisations of several countries.

2.1 Boom Clay

The Boom Clay Formation (Tertiary clay formation) is one of the potential clay formations studied in relation with the feasibility of a geological disposal of radioactive waste in Belgium. The Boom Clay dips gently towards the northeast, is located in the north part of Belgium and covers a surface of almost 5,000 km² (Supplementary Figure 1). The thickness of the formation increases from a few decametres at outcrop to more than 150 m in the deeper part of the basin. At the level of the URL in Mol (Belgium), the Boom Clay has a thickness of about 100 m and is located at depths between 185 and 287 m, the underground laboratory is at a depth of 223 m (Mertens et al., 2004). The total vertical stress and pore water pressure at the level of the URL in Mol are respectively 4.5 MPa and 2.2 MPa. The K_0 value ranges from 0.7 to 0.8 (Bernier et al., 2007a; ONDRAF/NIRAS, 2013).

The granulometry of the clay is composed of more than 60% of very fine particles (clay size) for the more clayey beds while there are 40% of clay particles for the more silty beds. The majority of the pores have a radius in the order of 0.01 μm with a unimodal distribution (Lima, 2011). Based on the differences in granulometry and mineralogical content, the Boom Clay Formation is subdivided in three members: the Belsele-Waas Member, the Terhagen Member and the Putte Member (Vandenberghé et al., 2014).

The vertical and horizontal hydraulic conductivity values are different with a ratio (k_H/k_V) of ~2 (Supplementary Table 3). The different values of the hydraulic conductivity are related with the granulometry, for instance, the values in the Belsele-Waas member are higher than those of the other members of the formation because of its higher sand content.

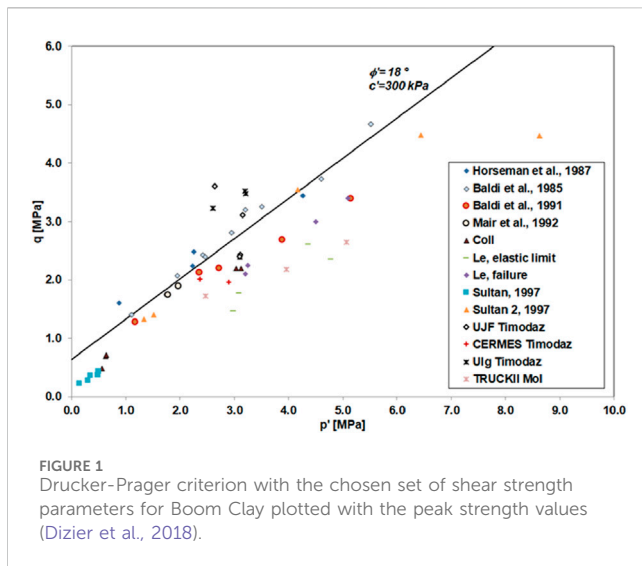
A critical review of the laboratory and *in situ* measurements can be found in Yu et al. (2013).

2.1.1 Hydro-mechanical behaviour

Since the operational start of HADES URL early in the 80s, many laboratory tests and *in situ* testing have been performed to understand the Boom Clay THM behaviour, among which triaxial and oedometer tests. Triaxial tests permit to determine deviatoric behaviour and then the strength parameters, while oedometer tests are more focused on the volume change behaviour. Clay samples have been studied in conditions as close as possible to their natural state around the HADES URL. As re-saturating Boom Clay samples at low confining pressure induces an important swelling that affects the microstructure and thus modifies clay properties (Coll, 2005; Sultan, 1997), Le (2011) suggested saturating Boom Clay at a confining pressure close to the *in situ* state of stress to minimise this swelling and disturbance of the clay.

The Boom Clay behaviour is characterised by a non-linear stress–strain response. Laboratory tests showed a trend of stiffness variation with strain level: its tangent stiffness at 0.01% deformation may be one order of magnitude larger than that at 1% deformation (Bernier et al., 2007a).

The elastic properties which govern the clay behaviour in the reversible domain of deformation have been determined with triaxial tests. According to Bernier et al. (2007a) the isotropic elastic modulus of the Boom Clay is about 300 MPa. This value was deduced by back-analysis of the *in-situ* measurements during



the excavation of the Test-drift obtained by Mair et al. (1992) and gives satisfactory results to model most of the triaxial tests on Boom Clay (Charlier et al., 2010). The value of the Poisson's ratio ranges from 0.125 (Bernier et al., 2007b) to 0.15 (Horseman et al., 1987). In isotropic condition, a value of 0.125 is commonly admitted.

The uniaxial compressive strength (UCS) of the Boom Clay is not well documented. According to Coll (2005), who determined the UCS on Boom Clay samples from a depth of 223 m, it should be around 2.5 MPa. Bernier et al. (2007a) reported a value of 2 MPa.

Triaxial tests to determine the shear strength parameters of the Boom Clay have been performed for several decades starting from De Beer et al. (1977). These results were mostly obtained through undrained tests because of the very low permeability of the clay. The monitoring of the pore water pressure permits to calculate the mean effective stress and to interpret the tests in terms of effective parameters. For example, results of undrained tests performed at very low confining pressure (high OCR) showed that the deviatoric behaviour presents a peak before a decrease (strain softening) till a residual strength (Supplementary Figure 2). The very low compressibility of the clay-water mixture implies that the volumetric deformation of the sample can be assumed theoretically as null. The representative stress path for such kind of tests is almost a straight line (Lima, 2011).

The values of the drained cohesion and the drained friction angle of the Boom Clay can be deduced from all the previous studies. According to Bernier et al. (2007a), who interpreted the tests of Baldi et al. (1987), Baldi et al. (1991) and Mair et al. (1992) with a Mohr-Coulomb criterion, the drained cohesion is equal to 300 kPa and the friction angle to 18°. Figure 1 presents the comparison between the Drucker-Prager criterion with the chosen shear strength parameters and the peak strength values from the triaxial tests on Boom Clay. With this set of parameters a relatively good agreement can be found for high values of the confining pressure, while for very low values, more discrepancies can be seen (ONDRAF/NIRAS, 2013; Dizier et al., 2018).

Concerning the volume change behaviour, Awarkeh (2023) summarised the results of oedometer tests performed on Boom Clay samples from Horseman et al. (1987) to Nguyen et al. (2013)

and gave a range of variation of the swelling index (C_s) between 0.05 and 0.15, of the plastic slope (C_c) between 0.25 and 0.40, and of the preconsolidation pressure between 5 and 6 MPa. The parameters present a large variation that can be explained by the natural variability of the clay and by the evolution of the test protocols, which are constantly evolving from the early tests.

With a view on the long-term volume change behaviour, Deng et al. (2012) performed oedometer tests with the purpose of studying the secondary consolidation behaviour of Boom Clay samples taken from two different locations. They found that the secondary consolidation coefficient (C_α) was positive during the loading paths and negative during unloading, with an average value of about 0.024, which agrees with the general classification criterion for clay soils of Terzaghi et al. (1996), where a range from 0.02 to 0.05 is given for shales and mudrocks. Similar results were obtained by Awarkeh (2023).

A set of laboratory tests was performed under different conditions to investigate the elasto-visco-plastic behaviour of Boom Clay under long-term deviatoric conditions (creep). Triaxial creep tests performed by Coll et al. (2006) and Chen et al. (2017) at ambient temperature evidenced the creep behaviour: the steady strain rate increased with the deviatoric stress level as observed for most other clay materials. Similar results were obtained more recently with the work of Awarkeh (2023). It was shown that the creep strain under a deviatoric loading starts at a certain value of deviatoric stress, which means that there is a threshold under which no creep can be observed.

The coupling between mechanical and hydraulic properties was studied by Horseman et al. (1987) and Coll (2005), who performed series of hydraulic tests on Boom Clay samples at different confining pressures and determined a trend in the evolution of the hydraulic properties with the mean effective stress. As expected, an increase of the applied load induced a decrease of the hydraulic conductivity. Coll (2005) also studied the effect of the deviatoric stress on hydraulic conductivity. Even if a discontinuity was initiated in the sample, no clear modification of the hydraulic conductivity was observed. Indeed, even if the permeability was modified locally around the cracks, this was not measurable at the scale of the sample. After shearing, the cracks were characterised by a very thin size which made difficult the description of the porosity along the localised shear band. Few years later, Monfared (2011) performed permeability tests before and after shearing and observed again that the shear band had no significant effect on the permeability of the sample, although—consistently with the results of Coll (2005)—very small variations of the permeability could be noticed. The interpretations given to these results differed in both studies though. Coll (2005) assumed that the shear band had a very local and insignificant effect on the global permeability of the sample, while Monfared (2011) made the hypothesis that the absence of permeability variation was the result of the self-sealing behaviour of the clay.

The laboratory test programme summarised above mainly investigated the THM behaviour of the Boom Clay as isotropic, so far the anisotropic behaviour of Boom Clay has not been much studied. Baldi et al. (1987) compared the calculated and measured volumetric strain during a triaxial test. Later, Labiouse et al. (2014) and François et al. (2014) performed hollow cylinder tests and presented their interpretations with anisotropic numerical models.

Different phases of loading and unloading were applied to the samples. Before and after unloading, the sample was submitted to microcomputerized tomography (μ CT) and particle tracking to determine the displacement of some specific points. The hole clearly converged after unloading, but the convergence was not homogenous and varied with the direction of the bedding plane, which resulted in anisotropic behaviour and a final eye-shape of the hole (Labouise et al., 2014). The radial displacements in hollow cylinder tests according to different directions was analysed by François et al. (2014), who found that they were not uniform, highlighting the anisotropic response of the clay. The higher displacement was parallel to the bedding plane, while the lowest one was perpendicular to the bedding. These results were confirmed more recently by Péguiron (2021). Also the back-analysis of the observed pore-water pressure variations in the far field of the HADES URL galleries during excavations and around the *in-situ* heater tests ATLAS and PRACLAY (see Section 3.1) support the idea that the THM behaviour of the Boom Clay is anisotropic (Charlier et al., 2010; Van Marcke et al., 2013). These last analyses reveal notably that perturbations in the far field—where deformations are small—can be much better represented by models when using different Young's moduli along the vertical and horizontal directions, with values generally larger than those summarised in Supplementary Figure 5.

2.1.2 Hydro-mechanical behaviour of the fractured/damaged claystone

During the SELFRAC project, tests were performed to study the self-sealing capacity of the Boom Clay, using different pore water chemistries to saturate the samples after the initiation of a fracture (Bernier et al., 2007b). The Boom Clay showed very good capacity of self-sealing (Supplementary Figure 3). Van Geet et al. (2008) performed permeameter tests on a fractured Boom Clay sample and monitored the evolution of the hydraulic conductivity with time to highlight the sealing process (Supplementary Figure 4). The hydraulic conductivity decreased with time, indicating the sealing process from a hydraulic point of view. Chen et al. (2014) showed that there is no positive or negative impact of the temperature on the sealing properties of Boom Clay by exposing samples (damaged and intact) to a heating cycle from 20°C to 80°C under constant volume conditions in a permeameter cell.

2.2 Callovo-Oxfordian claystone

The Callovo-Oxfordian (Cox) claystone consists of three major geological units, among which the argillaceous unit (UA) at the base is the thickest (from 100 to 120 m in the zone of interest). It is subdivided into three subunits (UA1, UA2 and UA3) with small and progressive variations. Subunit UA2 corresponds to the stratigraphic level where the clay content is higher and where the Meuse/Haute-Marne (MHM) URL experiments are carried out. The formation dips gently (average 1°) towards the northwest, the bedding plane can therefore be considered horizontal. The main level of the URL is located at a depth of 490 m.

The average porosity in the UA is 18%. The network of pores mainly comprises meso- and micropores with a predominant pore size of approximately 10–30 nm, and an extremely low connectivity

for pores larger than 40 nm. The texture is finely divided and is an assembly of tectosilicate and carbonate grains, connected by a fine matrix formed of clay minerals and calcite microcrystals. Both the tectosilicate and the carbonate grains show a preferential orientation of their long axis parallel to the sedimentation plane (Rebours et al., 2005; Robinet et al., 2012).

The water permeability is very low and ranges from 10^{-21} m² to 10^{-19} m², with a relatively low anisotropy (2–3 ratio). The stress regime in the area is anisotropic, with the major principal stress being horizontal and the ratio between the maximum and minimum horizontal stresses being at ~ 1.3 . For the calculations, at the URL level, the major horizontal stress σ_H is set at 16.1 MPa, $\sigma_v = 12.7$ MPa, $\sigma_h = 12.4$ MPa, and the pore pressure is 4.7 MPa. A geothermal gradient of 0.025 °C/m is estimated in the area, with a temperature of 22°C at 490 m (Gunzburger and Cornet, 2007; Wileveau et al., 2007).

2.2.1 Hydro-mechanical behaviour

The Cox claystone has a linear non-reversible (pseudo-elastic) behaviour at low levels of deviator stress (below 40%–50% of failure) and a non-linear behaviour beyond a level, with significant irreversible strains and slightly lower moduli. Brittle failure is observed at low confining pressures and a more ductile behaviour is seen at high confining pressure (over 21 MPa in the UA). Beyond a certain level of cumulative total strain, some residual strength is shown.

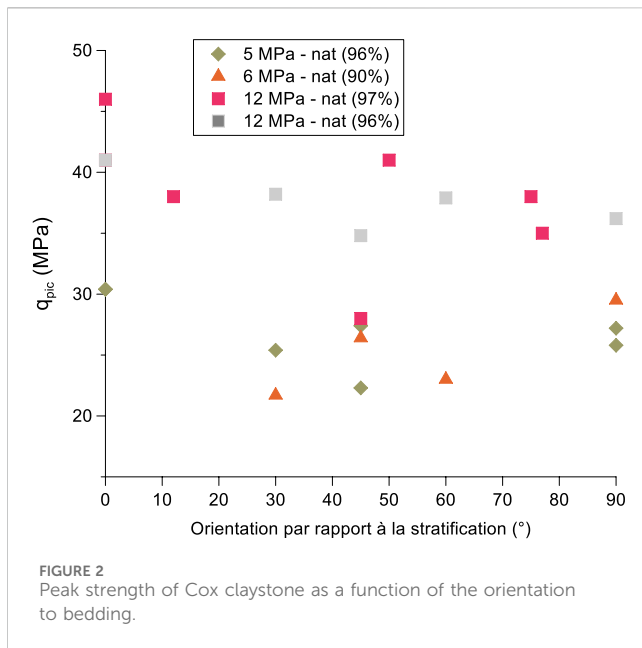
The water saturation has a significant effect on the mechanical behaviour of the Cox claystone. It was shown that limited desaturation of the Callovo-Oxfordian leads to an increase in the elastic mechanical properties and in the strength of the material, despite some microcracking of the sample due to desaturation (Wang et al., 2013; Agboli et al., 2024).

Under tensile loading, the Cox claystone shows a brittle behaviour. The measured tensile strength shows non-negligible dispersion, increasing with the carbonate content and with a mean value in the UA of 1.4 MPa.

Triaxial tests performed on samples with various orientations with regard to the bedding showed anisotropy, the $E_{//}/E_{\perp}$ ratio varying between 1.05 and 1.4. Similar numbers were obtained when calculating dynamic moduli from the compressive and shear wave velocities measured in both directions in parallelepipedic samples. The average values and standard deviations for the perpendicular and parallel moduli from UCS tests (calculated using the tangent method) in the UA unit were 5.7 ± 2.5 GPa and 11.0 ± 4.6 GPa, respectively. The average values show a ratio of almost 2, however these values are not directly comparable because many more samples were tested in the perpendicular direction (259 vs. 52). In addition, the standard deviation for the tests performed on samples parallel to the bedding (≈ 4 GPa) is related not only to the mineralogical variations, but also to the damage due to the difficulty to cut some plugs parallel to the lamination.

The Poisson's ratio (ν) calculated from all the results available at room temperature is on average 0.3 for all lithological levels.

The unconfined compressive strength in the different units of the Cox formation ranges from 18 to 34 MPa. For the most argillaceous part of the UA (UA2 = IMA subunit), the values are 23.3 ± 5.1 MPa.



The experimental results of uniaxial compression tests were interpreted with the [Hoek and Brown \(1980\)](#) failure criterion, and the values in [Supplementary Figure 2](#) were found. For the Cox claystone, the parameter σ_c (uniaxial compressive strength of the intact rock) is different from the UCS and is considered as a fitting parameter, not a rock property. In order to manage the uncertainties due to various effects (scale, time effect on the long-term strength, sample preservation, etc.) two criteria were defined: 1) an average criterion that goes through the cloud of test results over a range of confining pressure $0 < \sigma_3 < 25$ MPa, and 2) a low criterion that goes through the lower limit of test results over the same range of confining pressures. From these parameters the equivalent Mohr-Coulomb parameters shown in [Supplementary Figure 7](#) were derived.

Because of the variability of their microstructure and of their mineralogy, the Cox claystone has an anisotropic behaviour that results in:

- an anisotropy between 1 and 2 on the elastic moduli depending on the methods used for determination (dynamic and quasi-static modulus)
- compressive strengths measured on samples perpendicular to the stratification are similar to or slightly lower than those measured on samples parallel to the stratification. A decrease in strength was observed for test specimens at 45° but the natural variability of samples can give an opposite result. [Figure 2](#) shows the effect of the orientation to bedding on the peak strength in recent samples from well-preserved cores with high water saturations.

An investigation performed by [Zhang et al. \(2015\)](#) with cores drilled at different inclinations with respect to bedding, confirmed that the strength depends both on the loading path and on the direction of loading compared to the bedding plane. For a given loading orientation, the peak strengths developed during TCD (triaxial compression by axial deformation at constant radial

stress) and TCS (triaxial compression by axial loading at constant radial stress) were higher than those reached during TES (triaxial extension by increasing radial stress at a constant axial stress) and TEM (triaxial extension by keeping the mean stress constant while simultaneously increasing the radial stress and decreasing the axial stress) and the lowest strength was achieved in triaxial extension with constant mean stress. For all loading paths, the maximum strengths were reached with an axial stress parallel and perpendicular to bedding, and the lowest strength was obtained at 45° in compression and 30° in extension.

The very low permeability and porosity of the Cox claystone make it difficult to directly measure the pore pressure within a plug and to quantify its coupling with the mechanical behaviour. However, the hydro-mechanical coupling was revealed *in situ* through changes in pore pressure levels around the structures after excavation and through thermal experiments. It is currently described through the concept of effective stress using Biot's theory. The most recent experiments to define Biot's coefficient ([Braun, 2019](#); [Belmokhtar et al., 2017](#); [Yuan et al., 2017](#)) reduced the uncertainty on its value and gave higher values than previously, between 0.8 and 1 ([Supplementary Figure 5](#)). A value of 0.85 may be retained for the Cox claystone. However, it should be noted that these results strongly depend on the saturation and the mechanical state of the samples. The core processing, the sample preparation and the (re)saturation of the samples may create some damages prior to testing, which may partially explain the dispersion of experimental values. Furthermore, all the tests show that the Biot's coefficient seems to decrease with the confining pressure, while the drained bulk modulus increases. This could be explained by the closure of microfractures induced when cutting the core and/or preparing the samples. In addition, the very small pore size of the Cox claystone, the presence of both clay-bound and free water, and the possible induced desaturation when acquiring or preparing the samples hinder the characterisation of the poro-elastic parameters and the application of a simple behaviour model.

Creep tests were performed on dedicated rigs, with controlled temperature for periods of time of up to 3 years to characterise the long-term mechanical behaviour of the rock ([Zhang et al., 2012](#)). These tests faced important challenges related to the initial state of the samples, the duration of the experiments, the control of temperature and humidity and the precision of the measurements. The measured changes were indeed very low, sometimes of the same order of magnitude as the accuracy of the sensors. However, some general trends were observed:

- In most cases, the creeping rate diminished with time, although in some cases it appeared to reach an asymptote. The evolution of the creeping rate was very slow and because of the precision of the measurements, it is difficult to say whether a steady state was reached or not.
- The creeping rate appeared to increase with the deviatoric stress.
- The average stress seemed to have very little influence on the delayed deformations.
- The calcite content had a direct effect on the instantaneous behaviour but no clear trend was observed on the delayed

mechanical behaviour; however, when checking the results per study, a slight decrease of the creeping rate with the carbonate content may be seen.

2.2.2 Hydro-mechanical behaviour of the fractured/damaged claystone

The EDZ can be split in a connected fractured zone (ZFC), where both tensile fractures and shear fractures coexist, and a discrete fractured zone (ZFD), where only the ends of some shear fractures are found. For HLW cells drilled in the direction of the maximum horizontal stress, the EDZ develops mainly on the right and left sides of the borehole. Its maximum extent is approximately one diameter wide on each side (0.8 radius for the ZFC and 2 radii for the ZFD), and there is no “scale effect” between large galleries or thin boreholes. The hydraulic conductivity in the ZFC is significant and related to open fractures. Because of this, the pore pressure drops rapidly to atmospheric pressure in the near field (ZFC), but an increase in pore pressure is observed further away from the hole with some delay.

The apparent stiffness of the ZFC has been evaluated in the CDZ experiment (de la Vaissière et al., 2015): it appears to increase rapidly, reaching already 3 GPa 1 m away from the borehole wall.

Several observations in the UA showed that the EDZ has a hydraulic self-healing capacity due to the presence of swelling clay minerals such as smectite. Both laboratory and *in-situ* experiments showed that the hydraulic conductivity of the ZFC reduces rapidly when exposed to water and progressively reaches that of the intact claystone. De La Vaissière et al. (2015) showed the partial restoration of the Cox claystone permeability during *in situ* resaturation experiments. Over a 1-year resaturation period, the hydraulic conductivity measured in the boreholes decreased by up to four orders of magnitude, approaching, but not reaching, the value of the healthy claystone. This result illustrates the ability of the claystone to self-seal. However, water injection does not improve the stiffness of the EDZ, that remains a mechanically weak zone.

A study on Cox claystone looked at its flow properties (Cuss et al., 2017) and described the stress dependency fracture flow by a power-law or cubic relationship, which is likely to be dependent on the fracture roughness, thickness of gouge material, saturation state, permeability of the host material, and clay mineralogy (i.e., swelling potential). The stress-dependency of flow was also seen to be dependent on orientation with respect to bedding, in relation to the anisotropic swelling characteristics of Cox. Fractures perpendicular to bedding accommodated greater compression and resulted in a lower transmissivity.

2.3 Opalinus Clay

The Opalinus Clay is slightly tilted and the surface of the formation lies between 0 to beyond 1,000 m below ground surface. At Mont Terri, the Opalinus Clay reaches a maximum depth of about 1,000 m and the present burial depth is about 200–300 m.

On a regional scale, the mineralogical composition of the Opalinus Clay exhibits moderate lateral variability and a slight increase in clay content with depth. At the Mont Terri URL a clay-rich and a sandy facies can be identified. The variability of the facies is expected to be low and the same structures can be found in southern Germany as well (Jahn et al., 2016).

The anisotropy due to bedding is largely a result of microscopic heterogeneity. Porosity depends on clay content and burial depth. The pore space of the rock is formed by a network of micro/meso and macropores, but the majority of pores can be classified as mesopores (1–25 nm) (NAGRA, 2002a).

Field investigations suggest a hydraulic conductivity of the Opalinus Clay in the order of 10^{-13} to 10^{-14} m/s. No significant variations in hydraulic conductivity are seen among the different facies. A reference value of $5 \cdot 10^{-13}$ m/s has been reported for the Opalinus Clay at Mont Terri (Bossart and Thury, 2008). The water/air permeability experiments on the Opalinus Clay (NAGRA, 2002a; Marschall et al., 2005; Poller et al., 2007; Croisé et al., 2006; Romero and Gomez, 2013) show clear evidence for the dependency of water permeability on void ratio and thus on constitutive stress. A marked dependency of gas dissipation was observed on the direction of gas flow with respect to bedding orientation.

A compilation of water retention curves (WRC) of Opalinus Clay samples from Mont Terri, determined by GRS, UPC and EPFL is depicted in Supplementary Figure 6. Characteristic features of the Opalinus Clay are the high capillary pressures in the order of 10 MPa even at high water saturation >90% and the marked hysteresis between wetting and drying paths. Information about the WRC of deep Opalinus core samples (880 m depth) can be found in Ferrari et al. (2013) and Romero and Gomez (2013).

2.3.1 Hydro-mechanical behaviour

Geotechnical characteristics of the Opalinus Clay have been determined as part of comprehensive laboratory programmes, revealing moderate stiffness (Young’s modulus in the range 5–15 GPa), moderate strength (UCS values of the intact rock matrix between 10 and 35 MPa), distinct swelling pressures (0.5–2 MPa) and OCR of between 1.5 and 2.5 (NAGRA, 2002b).

Parameters of the Opalinus Clay as defined for the FE Experiment in Alcolea and Marchall. (2019) are shown in Supplementary Figure 8.

2.3.2 Hydro-mechanical behaviour of the fractured/damaged claystone

Experiments at BGS looked at fracture transmissivity in Opalinus Clay along an idealised fracture (Cuss et al., 2009; Cuss et al., 2011). A follow-on study investigated hydraulic flow along a realistic fracture (Cuss et al., 2012). This work showed that hydration alone reduced fracture transmissivity by one order of magnitude, while shear displacement reduced it by a second order of magnitude. Continued shear then resulted in increased flow, eventually increasing by five orders of magnitude, three orders of magnitude greater than the starting transmissivity. The injection of fluorescein showed that only around 25% of the fracture surface was conductive.

The values for the scoping calculations of the FE experiments used in Senger (2015) for the EDZ of the Opalinus clay are given in Supplementary Figure 10.

3 Relevant large-scale tests

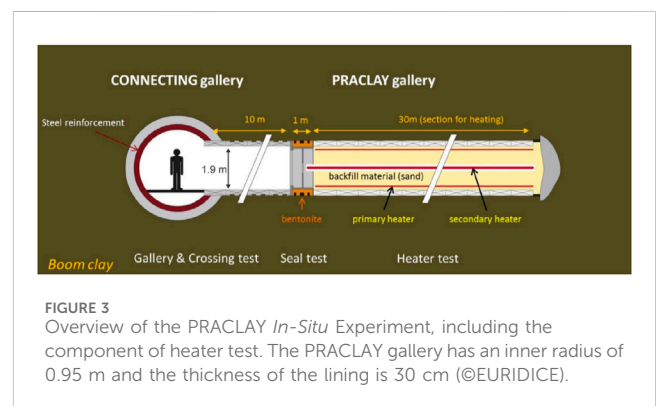
Several heating tests have been performed in underground research laboratories excavated in clay host rocks. The aim of these tests is usually to determine thermal properties of the host rock and help identify its hydraulic, mechanical and thermal

TABLE 1 Summary of relevant large-scale tests characteristics (BH: borehole).

Test	Duration	Characteristics	Heater temperature /Power	Dimensions	References
Boom clay (HADES, Belgium)					
ATLAS (I-IV)	1992–2008, in 4 phases	Small-scale heater test, simple geometry. One heater BH and 5 observation BHs with <i>T</i> , pore water pressure and stress measured	900–1800 W	8 × 0.19 m (BH)	De Bruyn and Labat (2002) Chen et al. (2011), Chen et al. (2023a), Chen et al. (2023b) Li et al. (2023)
PRACLAY Heater test	2014–2025	Large-scale heater test with a heated gallery filled with sand and closed by plug (hydraulic cut-off). Network of instrumented boreholes around (pore water pressure, <i>T</i> , total stress measured)	80°C (at the Boom Clay/ lining interface)	40 × 2.5 m (gallery)	Van Geet et al. (2007); Van Marcke et al. (2013); Dizier et al. (2021); Chen et al. (2023a, b); Li et al. (2023)
Cox (Bure URL, France)					
TER	2006–2009	Cyclic heating. <i>T</i> , <i>P</i> and strain measured in close BHs. Lab tests on core samples	300–900 W	3-m BH	Wileveau et al. (2007); Garitte et al. (2014)
TED	2010–2012	3 heaters. Focus on EDZ. <i>T</i> , <i>P</i> and strain measured in close BHs. Lab tests on core samples	90°C/600 W per heater	16-m BHs with 4-m heaters	Armand et al. (2017); Conil et al. (2020)
TFW	2011 (2 months)	Rapid heating. <i>T</i> and <i>P</i> measured	120°C–80°C/500 W	3-m BH	Armand et al. (2017)
ALC1604	2013–2019	Full-scale HLW cell	90°C/220 W/m	25-m BH with 15-m heated section	Tourchi et al. (2021); Bumbieler et al. (2021)
CRQ	2019, 2020	Rapid heating to reach thermal hydrofracturing. 10 heating BH, 2 heating phases	80°C–95°C/ 1750–2220 W	10 × 20 m BH with 10-m heaters	Plúa et al. (2023); Plúa et al. (2024)
ALC1605	2020–now	Full-scale HLW cell, annulus between casing and clay formation filled with MREA cement	85°C/220 W/m	25-m BH with 15-m heated section	Bumbieler et al. (2024)
CRQ2	2023	Rapid heating to reach thermal hydrofracturing. 10 heating BH	89°C/1750–2220 W	10 × 20 m BH with 10-m heaters	
Opalinus (Mont Terri URL, Switzerland)					
HE-D	2003–2005	2 heaters, 2 heating phases. <i>T</i> , pore water <i>P</i> , gas migration, deformation measured in 24 BH	100°C/650–1950 W	14 × 0.3 m (BH)	Wileveau (2005); Zhang et al. (2007); Wileveau and Rothfuchs (2007)
FE	2014–now	Buffer between heater and host rock	60°C–80°C	Real scale, gallery	NAGRA (2019)

responses to a thermal load thanks to the instrumentation inside or around the test. In the HADES facility excavated in Boom Clay, the small-scale ATLAS heater test was set up in 1992 with a very simple geometry (De Bruyn and Labat, 2002), and has undergone several phases, providing information on the temperature and pore water pressure evolution over the years, particularly in the far field (Chen et al., 2011; Chen et al., 2023). At the MHM URL, several *in-situ* heating tests on the Cox claystone have been performed since 2006, among which the TER, TED, TFW, ALC 1604 and CRQ. At the Mont Terri URL, the heating tests HE-E and FE, excavated in Opalinus Clay (described in the companion paper), are currently running. A summary of the main characteristics of these tests is given in Table 1.

The following sections describe in some detail the tests selected as modelling benchmarks in HITEC: the PRACLAY in Boom Clay and the ALC 1605 in Cox claystone.



3.1 Large-scale *in situ* PRACLAY heater test

The PRACLAY gallery was excavated in 2007 at the HADES URL and has a length of 45 m. The heated part of the gallery is 34 m

long and is separated from non-heated part by a hydraulic seal. The heated section of the gallery was backfilled with sand, saturated and pressurised with water after the installation of the seal in 2010. The main role of the seal is to hydraulically cut off the heated part from the non-heated part (Figure 3). Bentonite clay, which has a high swelling potential under hydration, was chosen to achieve this goal. In this way, the interface between the Boom Clay and the bentonite is sealed and permeability in the contact zone surrounding the seal is reduced. The high pressure inside the PRACLAY gallery is thus maintained.

The heating system consists of a primary heater, attached to the gallery lining, and a secondary heater, which is placed in a central tube that rests on a support structure. A control system regulating the heating power as a function of measured and target temperatures is also part of the heating system. During the start-up phase, the power was increased in a controlled manner to limit the thermal gradient over the gallery lining.

The heated part of the PRACLAY gallery is divided into three zones:

- Zone 1: front-end zone, 2.26 m long, close to the PRACLAY seal,
- Zone 2: middle zone, 28.48 m long, in the middle of the experimental part of the gallery,
- Zone 3: far-end zone, 3.29 m long, at the end of the gallery.

The power input can be controlled independently in each of the three zones. In this way, the end effects can be minimised and a temperature field that is as uniform as possible can be created along the heated section.

The sand that fills the gallery was put in place by blowing it in a dry state into the gallery before September 2011. Subsequently, a total volume of about 43 m³ of tap water was injected into this part of the gallery between January and May 2012. Saturation of the backfilled gallery was then naturally completed with the water flowing from the host Boom Clay into the gallery. The pore water pressure in the gallery gradually increased and after ~2.5 years it reached 1 MPa, and the backfilled PRACLAY gallery was estimated to be fully saturated. During the heating phase of the experiment, the pressure in the backfilled gallery evolves naturally without any human intervention (adding or subtracting an amount of water).

The PRACLAY *In-Situ* Experiment was intensively instrumented with about 1,100 sensors (piezometers, thermocouples, flat-jacks, strain gauges, etc.). Instrumented boreholes were drilled from both the Connecting gallery (CG) and the PRACLAY gallery (PG).

The heater was switched on the 3 November 2014 with a constant power of 250 W/m for the three zones of the primary heating system. Two months later, the power was increased from 250 W/m to 350 W/m. Finally, the power was again increased to 450 W/m and maintained until the temperature at the extrados of the concrete lining reached 80°C, 8 months after the start of heating. This temperature was kept constant by gradually reducing the power in the three zones. After 4 years of heating, the zone in which temperature was affected by the test extended up to about 15–20 m and continued to grow smoothly and slowly. The evolution of the temperature was seen to be slightly different between the horizontal

and the vertical directions, putting in evidence the anisotropy of the thermal conductivity. The pore water pressures in the experimental setup and in the clay also evolved smoothly, regularly and without any sudden or otherwise unexpected changes. The pore water pressure reached a value of 2.8 MPa in the backfilled part of the heated gallery and a maximum value of 3 MPa in the Boom Clay. In the far field, changes of pore water pressure were seen up to a distance of 22 m from the axis of the heated gallery, while the temperature had not increased at this location yet. At the end of 2023 the temperature at the interface between the Boom Clay and the extrados of the concrete lining was still maintained at 80°C.

More details about the large-scale *in situ* PRACLAY Heater test can be found in Van Marcke et al. (2013) and Dizier et al. (2021).

3.2 ALC 1605 HLW cell test

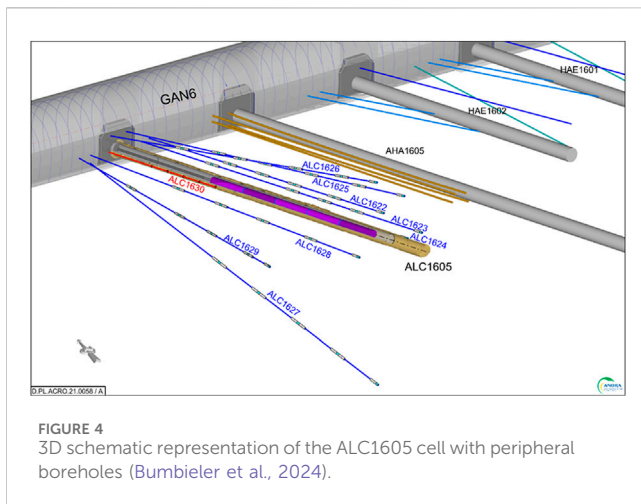
The ALC1605 full-scale heating experiment takes place in the MHM URL in north-eastern France. The 25-m long cell was drilled in the direction of the maximum horizontal stress from the GAN drift in November 2018. The characteristics of the cell correspond to the 2015 reference design of the Cigéo HLW cell, except for the length, which will be either 80 m or 150 m long. Compared to the previous full-scale heating experiment (ALC1604, Bumbieler et al., 2021), the 30" casing is now centralised and the annulus between the casing and the formation is filled with an alkaline cement grout called MREA (Matériau de remplissage de l'Extrados des Alvéoles). The MREA is injected in the annulus to reduce the corrosion rate of the casing by: (i) neutralising the acidic drainage produced by pyrite oxidation, (ii) reducing the amount of oxygen coming from the drift.

The detailed objectives of the experiment are to:

- Study the impact of a thermal load on the TM behaviour of the casing when the annulus is filled with an MREA cement.
- Study the impact of a thermal load on the THM behaviour of the Cox claystone in the near field (but beyond the EDZ) and in the far field (beyond a few cell diameters) with a filled annulus. The temperature and pressure evolution are monitored around the cell and at different offsets from the drift. A comparison with the measurements made during the ALC1604 experiment will help identify a potential impact of the filling material on the kinetics and the amplitude of the thermal pressuring in the near field, and possibly the far field.

The casing comprises thirteen interlocked elements, each measuring 2 m in length. Each casing element is equipped with temperature sensors on their inner surface, and five of them include convergence measurements to monitor casing ovalisation. Additionally, two casing elements are equipped with external fibre optics for strain and temperature measurements on the outer surface. In the formation, eight boreholes were drilled around the cell for pore pressure, temperature, and permeability measurements (Figure 4):

- 3 boreholes, diverging from the cell in a vertical plane with 5 measuring chambers and at least three of them in the heated zone;



- 4 boreholes in a horizontal plane on each side of the cell (2 of them diverging and 2 parallel to the cell) with 5 measuring chambers and at least three of them in the heated zone;
- 1 borehole parallel to the cell in a horizontal plane with 3 measuring chambers.

A last borehole called ALC1630, with five temperature sensors, was drilled parallel to the ALC1605 cell.

The cell is heated over 15 m by five heating elements, providing a power of 220 W/m. After a low power test in March 2020, the main heating phase started in June 2020. The heating power history from ALC1604 experiment was replicated to help comparing the two concepts (with and without filled annulus). After 3 years of heating in June 2023, the casing temperature was reaching 85°C in the upper side of the casing (Supplementary Figure 7). The main heating phase is planned to last at least 5 years, until 2025.

4 Effect of temperature on clay host rocks

4.1 Background

The thermal phase of a repository has consequences on 1) the clay behaviour around galleries, 2) the extent of the excavation damaged zone (EDZ), and 3) the clay properties within that EDZ. In turn, the THM behaviour of the clay is characterised by several coupled processes. As recalled in a synthesis by Li et al. (2023) on the THM behaviour of Boom Clay, the behaviour of clay submitted to heat is mainly governed by the coupling between the solid skeleton, the clay particles and the fluid phase.

The value of the thermal expansion coefficient of water is more than ten times greater than the value for the rock matrix. This large difference is the main cause of thermal pressurisation. The volumetric dilation of a solid is much lower than that of the fluid phase (water) filling the pore space. As a consequence, the fluid phase dilates more than the solid phase during heating and tends to occupy more space. Hence, the temperature rise in a low permeability porous medium, such as Callovo-Oxfordian and Opalinus claystones, generates a pore pressure increase. This

excess pressure reduces the effective stresses and may cause the failure of the sample. Among the usual constituents of the clay host rocks, the coefficients of the clay and quartz are similar, but those of calcite and feldspar are almost three times lower. This may also trigger some thermal damaging, especially at the interface between calcite and the clay matrix. Nevertheless, the competition between excess pore pressure due to thermal pressurisation and drainage due to pore pressure gradient increase is the key mechanism for the potential damage induced by the heat emitted from the waste.

High temperatures may also cause permanent damage to the EDZ, impacting the self-sealing capacity of the rock, and alterations in hydro-mechanical behaviour caused by prolonged heating. The ability of claystone to self-seal has been proven by several authors (see sections 2.1.2 and 2.2.2), and some processes involved (such as intraparticle swelling due to crack resaturation, inter-particle swelling due to osmotic effects, and plugging of fracture by particles aggregation) have been identified. Throughout the TIMODAZ experimental programme no evidence was found showing temperature-induced additional opening of fractures or a significant permeability increase of the EDZ. Instead, the thermal-induced plasticity, swelling and creep of clay are likely beneficial to the sealing of fractures and recovery of the permeability of the EDZ to the original state of the clay host rock (Yu et al., 2010).

Other findings of the TIMODAZ project were that in the absence of plastic deformation, elevated temperatures do not seem to adversely affect the pore structure of the clay, since the intrinsic permeability remains constant or even decreases with the increase of temperature. Temporary increases of hydraulic conductivity of clay could be explained entirely by the decrease of water viscosity and would be therefore reversible with temperature. Where thermo-plasticity was observed, thermo-consolidation was most likely to occur resulting in a void ratio and intrinsic permeability decrease.

4.1.1 Thermo-hydro-mechanical behaviour of Boom Clay

The thermal dissipation in a medium can be defined by two parameters, the thermal conductivity, which defines the dissipation of heat, and the volumetric heat capacity, a storage parameter. Djéran (1991) performed laboratory experiments with a needle probe to determine the thermal conductivity (λ) and the volumetric heat capacity of the clay. Buyens and Put (1984) estimated the different thermal parameters by back calculation of an *in-situ* experiment in the quarry of Terhagen. Later, the *in-situ* heater test ATLAS conducted at the HADES URL allowed the determination of the thermal conductivity in different directions. All these values are summarised in Supplementary Table 10. These results show that depending on the test conditions (laboratory, *in situ*) different values of the thermal conductivity can be found. Djéran (1991) explained these differences by the induced swelling due to the removal of the *in-situ* stress that can disturb the sample and modify the contact between the clay particles. As a consequence, a possible modification of the density may occur resulting in a change in the thermal conductivity. Dao (2015) measured the thermal conductivity in clay samples located at different distances from the wall of the connecting gallery. A decrease of the thermal conductivity in the first metres from the wall was observed. This decrease may be linked to a modification of the

fundamental properties of the clay induced by excavation and so by the release of the confining pressure.

Hueckel et al. (2009) performed undrained triaxial tests on normally consolidated Boom Clay where one sample was heated at a given deviatoric stress. The excess pore water pressure induced in the heated sample followed a stress path towards the critical state line, leading to the failure of the sample. During the TIMODAZ project (Delage et al., 2010), Monfarred (2011) showed that undrained heating can be responsible for the reactivation of a pre-existing shear band during thermal pressurisation of a hollow cylinder in Boom Clay.

The mechanical behaviour of Boom Clay submitted to heating/cooling phases has been studied for a long time (Baldi et al., 1987; Baldi et al., 1991; Sultan, 1997; Cui et al., 2000; Delage et al., 2000). Contractive/dilatative behaviour was observed in drained heating tests at different confining pressures by Baldi et al. (1991) and Sultan (1997). For normally consolidated and slightly overconsolidated samples, the behaviour remained contractive during the heating phase, while for highly overconsolidated samples dilation was followed by contraction.

In addition to this dilatative/contractive behaviour, clayey soils undergo variation of their elastic limit with temperature. In the case of fine grained soils, the preconsolidation pressure decreases with the increase in temperature. Le (2011) obtained in two oedometer tests a preconsolidation pressure of 5 MPa at ambient temperature and of 4 MPa at 80°C. Also, when a clay sample is submitted to temperature increase, an overconsolidation effect occurs. This was observed by Cui et al. (2000) during isotropic compression of Boom Clay samples when the clay was heated at a constant pressure and then reloaded at a higher temperature.

The hydraulic conductivity is also affected by temperature, and more specifically, the viscosity of water decreases with the increase of temperature. As a consequence, the hydraulic conductivity will normally increase with temperature (e.g., Delage et al., 2000; Lima, 2011). This change in water viscosity with temperature only affects the hydraulic conductivity of the clay, but not its intrinsic permeability, as experimentally shown by Delage et al. (2000) and Lima (2011).

Djéran (1991) performed tests to study the influence of temperature on creep and showed that at high temperature the rate of creep seems to increase: the clay became more ductile and viscous. The thermal effect on secondary compression was analysed by Cui et al. (2009). With the increase of temperature, the strain rate increased more with time than at ambient temperature, i.e., the consolidation rate increased with temperature.

4.1.2 Thermo-hydro-mechanical behaviour of Callovo-Oxfordian claystone

The thermal conductivity of the UA was both measured on samples taken in boreholes drilled for the TED experiment and determined by inverse analysis during this experiment (Tourchi et al., 2019). The results obtained with both approaches matched very well (Supplementary Table 11), which shows that there is no scale effect and that laboratory measurements can be used to characterise the thermal behaviour of the Cox claystone.

The thermal and THM modelling of the TED experiment using the parameters in Supplementary Table 11 matched well the evolution of temperature during the whole heating phase,

showing that thermal conductivity does not vary with temperature. This point was also proven by laboratory measurements: for tests performed at temperatures between 20°C and 150°C, the horizontal and vertical thermal conductivities were almost independent of temperature, whereas there was a clear increase of the conductivity with the water saturation (Jobmann et al., 2013).

Specific heat measurements performed on samples from four different boreholes showed that it does not vary much with depth. In the UA, the average value at 20°C is 973 J kg⁻¹·K⁻¹. Inverse analyses from the TED experiment gave 971 and 987 J kg⁻¹·K⁻¹.

Although there is no direct measurement of the thermal properties of the EDZ, they have been estimated by inverse analysis of the temperatures measured during the ALC1604 HLW cell heating test (Tourchi et al., 2019). The 3D modelling of the experiment matched well the temperature measurements using the same conductivity in the EDZ as in the intact rock. A sensitivity study showed that the temperature field beyond the EDZ is very weakly influenced by the thermal properties of this zone. It appears therefore justified to use the same conductivity in the EDZ and in the intact Cox claystone.

The undrained thermal expansion coefficients (α_u) parallel and perpendicular to bedding found in laboratory tests performed on samples as part of the TED *in-situ* experiment were $10.2 \pm 1.9 \cdot 10^{-6} \text{C}^{-1}$ and $18.2 \pm 4.9 \cdot 10^{-6} \text{C}^{-1}$, respectively. The drained linear thermal expansion coefficients (α_d) obtained by Braun (2019) parallel and perpendicular to bedding were $0.5 \cdot 10^{-5} \text{C}^{-1}$ and $0.2 \cdot 10^{-5} \text{C}^{-1}$, respectively. These values are lower than the ones obtained in undrained conditions and the one used by Tourchi et al. (2019) in their inverse analysis of the TED experiment ($1.3 \cdot 10^{-5} \text{C}^{-1}$), but all remain much lower than the coefficient for water. Tourchi et al. (2019) showed that this parameter does not have much influence on the pressure variations.

The effect of temperature on various THM parameters was studied in the 25°C–80°C range (Zhang et al., 2012). The elastic modulus showed a very slight tendency to decrease as the temperature increased, although this reduction could also be attributed to the mineralogical variability between samples. The stress at failure decreased slightly with the increase in temperature and this phenomenon was more pronounced for low confinement values.

Several authors (Baldi et al., 1991; Delage et al., 2000) showed that normally consolidated clays subjected to constant mechanical load and slow temperature increase generally experience irreversible contraction. Weakly overconsolidated clays experience first thermal expansion, followed by contraction. This phenomenon is interpreted by a variation in the elasticity limits with temperature called “thermal hardening”. Cox samples exhibited thermo-elastic expansion up to a temperature around 45°C, followed by thermo-plastic contraction at higher temperature that could be enhanced by the appearance of microcracks resulting from some desaturation of the samples (Belmokhtar et al., 2017).

Braun (2019) performed a series of tests under thermal load in drained conditions. The contraction was essentially localised perpendicularly to bedding, whereas the strains parallel to bedding were reversible and linear. In this direction, the samples expanded when heated, and contracted when cooled down, showing that the response to thermal loading is thermo-elastic

(Supplementary Figure 8). Perpendicular to bedding, the rock expanded up to 40°C, then contracted for higher temperatures. While cooling, linear contraction was observed. This phenomenon was not observed in small-scale *in situ* experiments such as TER or TED, where measurements were performed in the far field. However, the full-scale ALC1604 experiment showed in some cases a “relaxation” of the radial load applied by the rock on the steel casing, that could be a sign of thermal hardening in the EDZ.

The change of pore pressure may be related to the applied temperature variations by the thermal pressurisation coefficient. This coefficient depends on the nature of the rock, the range of temperature variation, the level of damage of the material, and the state of stress. A special isotropic cell was designed to conduct thermal pressurisation tests under stress conditions close to the *in situ* state (Tang et al., 2008; Mohajerani et al., 2012). With the same device, Braun (2019) performed two heating tests in three phases with application of thermal load. The resulting thermal pressurisation coefficients (see Supplementary Figure 9) are consistent with the theoretical values, they increased from 0.12 MPa/°C at 25°C to 0.30 MPa/°C at 80°C, whereas the values by Mohajerani et al. (2012) were almost constant. The stress conditions during the experiments explains this difference: Mohajerani et al. (2012) did not maintain constant effective stresses and their reduction led to a decrease in the Biot modulus and a practically constant thermal pressurisation coefficient.

Temperature may play a role in the long-term behaviour of the Cox claystone. Pellet (2007) reviewed the studies performed on time-dependent deformation and found that, despite the large dispersion of data, the deviator stress had a clear influence on the creep rate, whereas the effect of temperature overall was not obvious. Zhang et al. (2010) performed uniaxial compression tests under two different confining pressures (0.74 and 13.8 MPa) and a series of triaxial tests with a constant axial stress (15 MPa) but different radial stresses, 3.1 and 5 MPa. During these tests, temperature was increased and decreased in steps. This led to a slight increase in deformation due to thermal expansion, followed by a resumption of the creep. The higher temperature caused in general an increase of the deformation rate (up to 5 times larger), which may be related to the decrease of viscosity with temperature.

Auvray et al. (2015) performed self-sealing tests on the Cox argillite in a PEEK triaxial cell under room temperature, with 2D X-ray scans. Giot et al. (2019) performed the same kind of tests with 3D X-ray scans but with a limited amount of data and basic voxel data analysis.

4.2 Progress made during HITEC

During the HITEC project two aspects were mainly analysed: the impact of temperature on the short- and long-term behaviour and the self-sealing processes. In the first case the focus was on the thermal pressurisation and the risk of damage when the effective stress increases up to the overburden weight. In the near field, characterised by a fractured zone, thermal pressurisation could induce fracture opening or propagation in the EDZ, altering its permeability. In the far field, this could induce rock damage and reactivate fractures/faults (if they exist).

Furthermore, fractures subject to water circulation in clayey rocks can fully or partially close, leading to self-sealing processes. The availability of water within the EDZ may change over the timeline of a repository and therefore self-sealing of fractures could occur at a time where the repository is producing elevated temperatures. The swelling phenomena of the material around the lips of the crack are sensitive to water re-saturation, they could also be sensitive to temperature: geometric characteristics (opening and volume) and permeability of fractures could evolve as a function of temperature.

4.2.1 Hydro-mechanical behaviour

The short-term effect of temperature on the mechanical behaviour of the Callovo-Oxfordian claystone was analysed by compression tests performed at the University of Lorraine in a triaxial cell with strain measurements at different temperatures (20, 40, 60, 80, 100°C and 150°C), confining pressures (0, 4 and 12 MPa) and sample orientations (parallel and perpendicular to the bedding plane) (Grgic et al., 2023a). The tested samples were initially a little unsaturated (degree of saturation between 90% and 97%) and the compression tests were performed under the so-called pseudo-drained condition, with the drainage circuit of pore fluid open and connected to the atmospheric pressure. Indeed, with respect to the small size of samples, the selected strain rate (5·10⁻⁶/s) is considered slow enough to avoid significant over-pressurisation of the pore fluid. The analysis of elastic coefficients from the short-term compression tests indicated that in all cases an anisotropic damage developed during the deviatoric loading due to the opening of axial microcracks. This result had already been observed in previous works and was confirmed here on the Cox claystone at high temperatures. In addition, the peak deformation and strength increased when confining pressure increased. The initial heating stage generated a transitory pore water overpressure due to thermal expansion (because of the rapid thermal loading rate), which created microcracks probably parallel to the bedding plane. Despite the scattering of results, an overall decrease of the peak strength with increasing temperature (until 100°C) was observed because of the THM damage induced by the initial heating (Figure 5). For the parallel samples under uniaxial conditions, this decrease was the most important and volumetric dilatancy developed during loading for the highest temperatures. For all other conditions, the decrease was more moderate and there was no dilatancy because the confining pressure reduced the creation of initial thermo-induced microcracks. Hence, a lower thermal loading rate would have induced a lower overpressure and probably a much lower damage. The microcracks were closed when the axial stress increased during the compression tests when the orientation was perpendicular. There was no noticeable impact of temperature up to 100°C on the evolutions of the elastic coefficients. The peak strength increased at the highest temperature (150°C) in all cases due to the water vaporisation and consequently strong desaturation of the samples, which induced the development of a very significant capillary suction.

BGS undertook a series of oedometric (K_0) experiments measuring the spatial and temporal development of pore water pressure caused by thermal expansion and its subsequent impact on the evolution of intrinsic permeability (reported in Grgic et al., 2023a). Samples of clay/mudrock were tested from ambient to 90°C

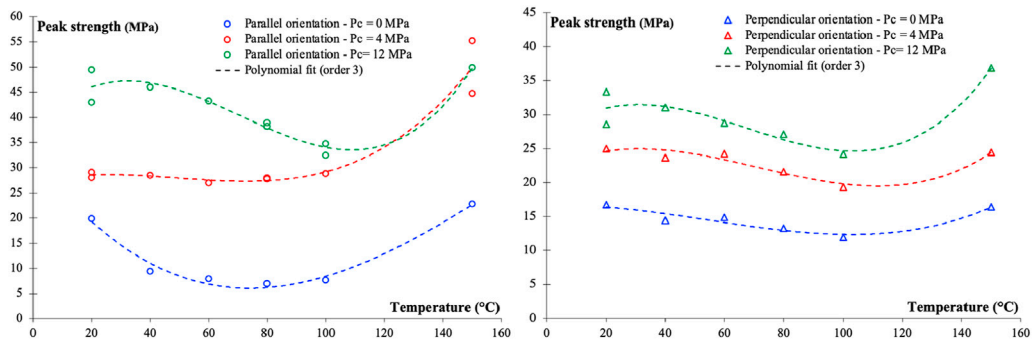


FIGURE 5 Evolution of the deviatoric stress at peak (peak strength) as a function of temperature for parallel (left) and perpendicular (right) orientations and for various confining pressures (Gbewade et al., 2024).

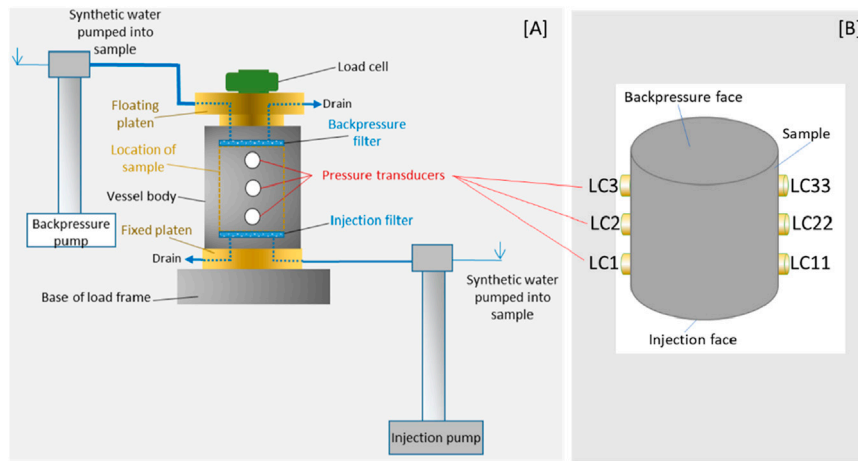


FIGURE 6 Schematic showing the layout of the BGS key apparatus components (A) and the position of the pore pressure sensors (B) around the periphery of the sample (Grgic et al., 2023a).

for orientations both parallel and perpendicular to bedding. A bespoke apparatus was specifically designed (Figure 6). After rehydration with synthetic solutions permeability was measured. The temperature designated for a particular test was then applied in a single step, and the development of overpressure was monitored along with the thermal expansion of the sample. Permeability was measured during this phase and after final cooling. Backpressure was between 2 and 4.5 MPa, injection pressure between 2 and 6 MPa and the axial stresses between 4 and 14 MPa.

In all cases permeability decreased with the increase of effective stress and on heating, with the rate of change linked to the initial permeability of the sample (Figure 7). The observed drop in permeability with temperature could be explained by the thermal contraction of the OPA by a small amount. As expected, permeability was lower perpendicular to bedding, with anisotropy ratios ranging from around 2.1 to 3.3 at 25°C and 85°C respectively. Only one Cox sample was tested and its permeability ($7.10 \times 10^{-21} \text{ m}^2$) was considerably lower than that of Opalinus (and in contrast to the numbers reported in Supplementary Tables 3, 5 that take also into account the measurements acquired in *in-situ* experiments), leading

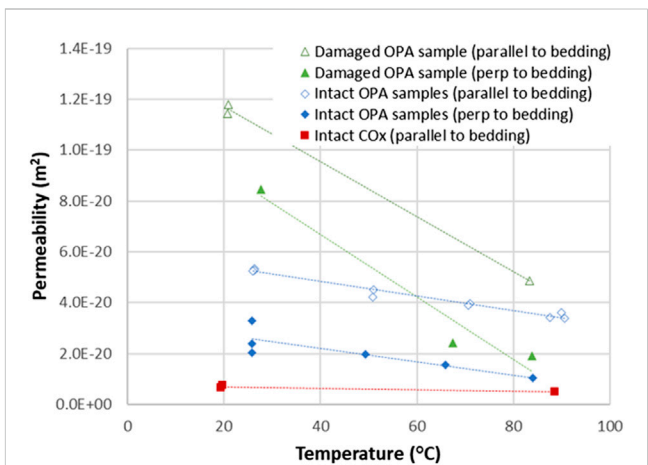
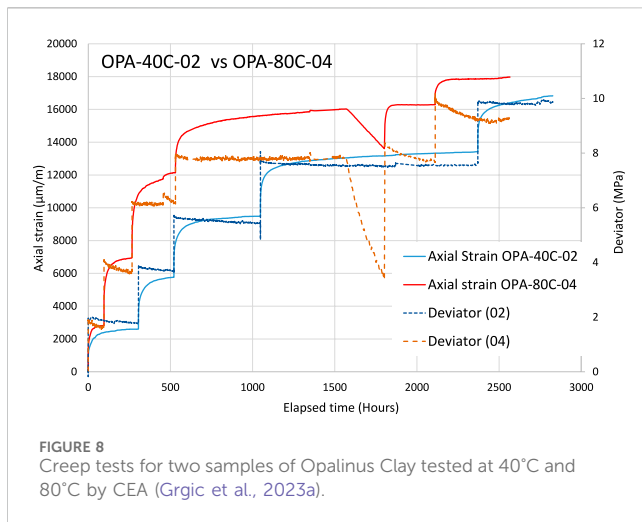


FIGURE 7 Permeability for OPA and Cox against temperature obtained by BGS (Grgic et al., 2023a).



to higher peak pore water pressures and possible evidence of thermally induced mechanical failure. However, in all experiments, no evidence for the degradation of hydraulic properties was observed once temperatures had dissipated.

In all tests, the pulse in pore water pressures caused by heating of the sample was short-lived (<24 h), reflecting the stiffness of the materials and the small amounts of water moved due to thermal expansion/contraction. In Opalinus Clay, heating to temperatures of 70°C and upwards resulted in the development of local pore water pressures exceeding the axial stress, with peak pressure increasing with temperature. However, in the test performed at elevated axial stress, peak pore water pressures remained below axial stress. This suggests that while the development of internal pore water pressure is linked to the heat applied and the permeability of the material, the magnitude of the effective stress is also important in limiting the potential for localised thermally-induced hydraulic damage. Porewater pressures exhibited local anisotropy (measurements of pore pressure on the same plane of a sample at locations 180° apart were different) and possible heterogeneity effects (variability in the response between individual samples prepared with the same bedding orientation, for example, differences in the magnitude of the peak porewater pressures) at least on the length scale of the experiments.

To analyse the long-term behaviour a series of multi-step creep tests were performed on Opalinus and Boom Clay under constant elevated temperature by CEA (reported in Grgic et al., 2023a). Samples taken from close positions along a core were first saturated under isochoric conditions and at room temperature with solutions representative of the clay pore water in triaxial cells. Then each sample was heated to a different temperature and the deviatoric stress was increased by steps, keeping constant the confining and pore pressures (confining pressure 4.7 MPa and pore pressure 2.2 MPa for Boom Clay, confining pressure 6 MPa and pore pressure 2 MPa for Opalinus Clay). The natural variability of the samples hindered a straightforward comparison of the effect of temperature, but for Opalinus clay, the magnitude of the strain for a given deviatoric stress was more important when the temperature was higher (Figure 8). Moreover, the kinetics of the strain development was faster for the higher temperature. During some steps under a great deviatoric stress failure occurred.

4.2.2 Self-sealing

During HITEC the self-sealing process in the Callovo-Oxfordian claystone was analysed at the University of Lorraine by performing self-sealing tests with water injection on initially (artificially) fractured cylindrical samples under different temperatures, sample orientations (parallel and perpendicularly to the bedding plane), calcite contents and initial crack openings (Grgic et al., 2023b). Self-sealing tests were performed in a novel mini-triaxial compression cell made of PEEK CF30 transparent to X-rays which made it possible to follow the evolution of the crack volume in the sample at different times under a high-resolution X-ray computed tomography (CT) scanner (Supplementary Figure 10). 3D scans were performed on all tested samples before, during and after the experiments. These self-sealing tests were performed under a confining pressure of 4 MPa. Water permeability was measured continuously during all tests.

Overall the self-sealing process was fast at the beginning of the tests and stabilised after 1 month (Figure 9). Thanks to the self-sealing process, the permeability of the Cox claystone samples (Figure 9, right) was partially restored ($\sim 10^{-18}$ – 10^{-19} m²) compared to the initial permeability of the healthy (i.e., without fracture) claystone ($\sim 10^{-20}$ – 10^{-21} m²). The mineralogical composition of the Cox claystone influenced the self-sealing process: the higher the calcium carbonate content (and therefore the lower the clay content), the less effective the self-sealing process, whatever the sample orientation. To have an effective sealing, a carbonate content lower than 40% was necessary (Figure 10). No significant influence of the sample orientation on the self-sealing kinetics was identified at this stage; the self-sealing process was equally efficient for both parallel and perpendicular orientations. In contrast, the opening of the initial artificial crack did influence the kinetics of the self-sealing process: it was faster for an initial crack opening of 0.4 mm than 0.8 mm. Finally, temperature may have a slight delaying effect on the self-sealing process, since the volume of the crack decreased more slowly at higher temperature (80°C). However, the permeability reduction did not seem to be impacted by temperature.

The University of Grenoble developed a cell to be used on the D50 beamline from ILL (Grenoble) for dual X-ray and neutron tomography and with a temperature control up to 90°C. Cylindrical specimens (centimetric size) were cut from *in-situ* collected cores and prepared with a synthetic crack in the middle axial plane. The crack was initially open and the specimen placed in oedometric conditions (no radial displacement of the outer boundary). Neutron and X-ray scans were done every 15 min during the flow of synthetic host pore water through the crack (Figure 11). Crack closure, local swelling around crack and water re-saturation (water content evolution) were quantified thanks to the neutron and X-ray scans and DIC analysis based on Stavropoulou et al. (2020). Tests were performed at three different temperatures on samples parallel and perpendicular to bedding. Although the tests conducted had a very short duration, it was possible to observe some features of behaviour. At 25°C, quasi-instantaneous closure of the crack was favoured by the formation of a dense network of micro-cracks sub-parallel to the bedding in the area close to the interface lips, creating a highly damaged material that filled the interface space. At 90°C, the mechanism was more diffuse and secondary

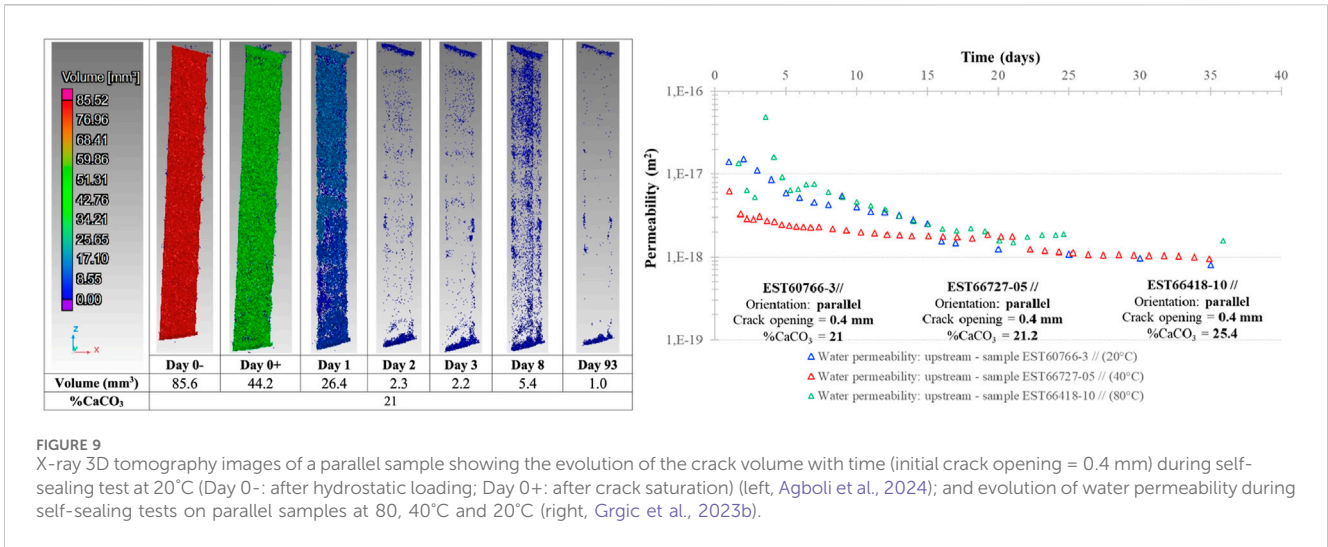


FIGURE 9 X-ray 3D tomography images of a parallel sample showing the evolution of the crack volume with time (initial crack opening = 0.4 mm) during self-sealing test at 20°C (Day 0- : after hydrostatic loading; Day 0+ : after crack saturation) (left, Agboli et al., 2024); and evolution of water permeability during self-sealing tests on parallel samples at 80, 40°C and 20°C (right, Grgic et al., 2023b).

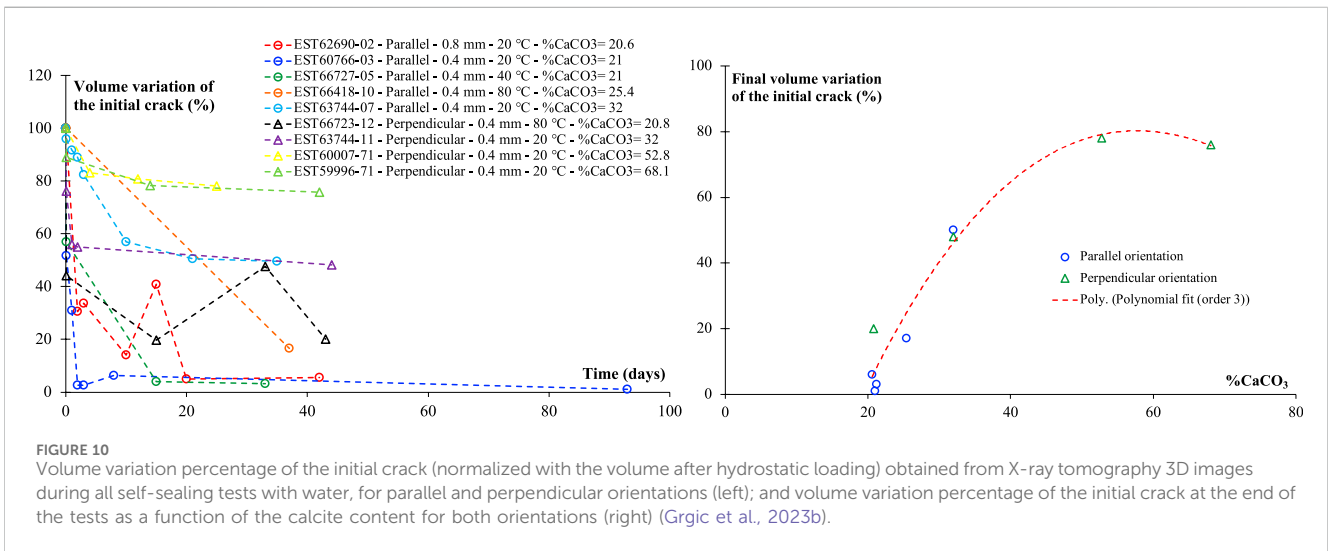


FIGURE 10 Volume variation percentage of the initial crack (normalized with the volume after hydrostatic loading) obtained from X-ray tomography 3D images during all self-sealing tests with water, for parallel and perpendicular orientations (left); and volume variation percentage of the initial crack at the end of the tests as a function of the calcite content for both orientations (right) (Grgic et al., 2023b).

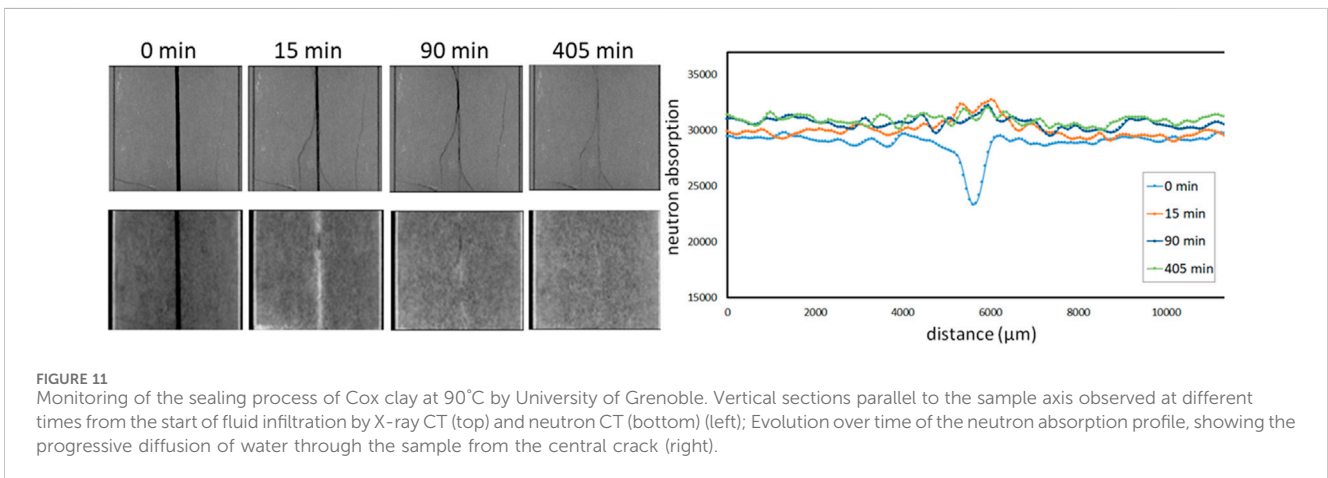
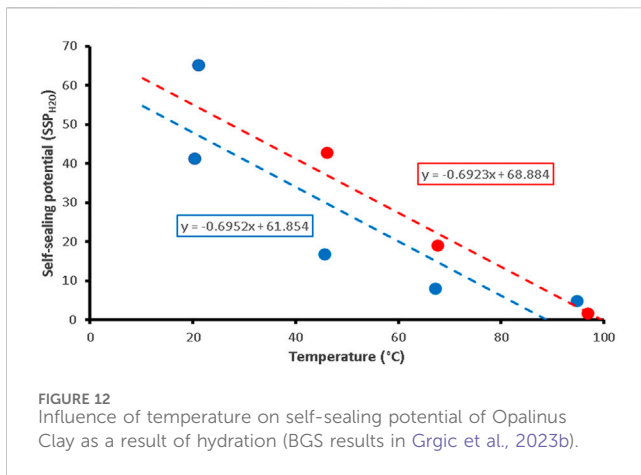


FIGURE 11 Monitoring of the sealing process of Cox clay at 90°C by University of Grenoble. Vertical sections parallel to the sample axis observed at different times from the start of fluid infiltration by X-ray CT (top) and neutron CT (bottom) (left); Evolution over time of the neutron absorption profile, showing the progressive diffusion of water through the sample from the central crack (right).

cracks were scattered. Hence, the re-closure kinetics was more gradual and greater in intensity at 90°C, favoured by a diffuse swelling in the whole sample. In both cases, the interface with an

initial opening of around 0.3 mm was completely filled within around 3 h, although the mechanisms were slightly different, showing a more ductile character at 90°C.



BGS performed a series of novel experiments using a highly instrumented bespoke direct shear apparatus, the Heated Shear Rig (Supplementary Figure 11, described in, e.g., Cuss et al. (2011)), using heating cartridges and band heaters attached to the rig to increase temperature up to 90°C. The samples, prepared by machine lathing, were 60 ± 0.01 mm in diameter and 53 ± 1 mm in height. The intact samples were initially sheared, then hydraulic flow was imposed into the fracture, and finally active shearing took place under constant hydraulic flow. The results reported in Grgic et al. (2023b) showed that temperature has a considerable effect on the shear properties of Opalinus Clay and Cox.

All tests with Opalinus Clay showed elastic-brittle behaviour, with peak shear stress increasing by 0.47 MPa per 10°C temperature. Residual strength also increased with temperature at a rate of 0.09 MPa per 10°C. Shear modulus showed considerable spread in the data, but also showed an increase with temperature. Repeat shear in Opalinus Clay also showed a clear increase in peak strength of 0.175 MPa per 10°C and residual strength of 0.178 MPa per 10°C. A small increase in shear modulus was seen but with considerable spread in the data. Therefore, in intact and re-sheared Opalinus Clay, strength and compliance increase with temperature. The increase was greater in intact OPA.

Considerable variation was seen in the flowrate into the fracture that could not be described by fracture surface characteristics. Therefore, two different self-sealing potential (SSP) coefficients were defined: a) as a result of hydraulic flow along the fracture (SSP_{H_2O}); b) as a result of active shear along the fracture while hydraulic flow continued (SSP_r). The SSP coefficient describes the proportional change in flow as opposed to the absolute change in flowrate. Self-sealing potential was seen to change with temperature in Opalinus Clay. A clear relationship was seen with SSP_{H_2O} , with a reduction in self-sealing capacity with increasing temperature (Figure 12). At a temperature of 90°C, the self-sealing potential was negligible. A difference was seen between SSP_{H_2O} for fractures that were formed at ambient temperature and those formed at temperature, although this may simply be explained by natural variation between samples. This result suggests that SSP_{H_2O} is better in fractures that have formed at temperature. This may be related to differences in fracture topology. Considerable spread of results was seen for self-sealing potential because of active shear (SSP_r). However, a reduction in SSP_r was seen with increasing temperature. In conclusion, for Opalinus Clay, the effectiveness of self-sealing processes reduced at elevated temperatures.

All fracture surfaces were laser scanned following the initial and re-shear stages of the experiment. Little variation was seen in roughness characteristics for the initial shear samples, with a reduction in roughness seen during re-shear. Little variation was seen in fracture topology for shear fractures created at different temperatures in initially intact samples. The presence of water during the re-shear phase resulted in the reduction in fracture roughness. As self-sealing potential (SSP_{H_2O}) is a function of temperature and fracture roughness alters with temperature, it is likely that fracture roughness played a role in the effectiveness of fractures to self-seal.

In the tests performed with Callovo-Oxfordian claystone by BGS the stress-strain response showed a similar form over the full range of temperatures, although as temperature increased the response was more brittle. Peak strength was seen to increase by 0.13 MPa per 10°C, with residual stress increasing by 0.01 MPa per 10°C. Shear modulus reduced with temperature, although this result may be influenced by a low modulus seen at the highest temperature. Callovo-Oxfordian claystone therefore increases in strength with temperature but has a reducing stiffness. Self-sealing processes in Callovo-Oxfordian claystone were seen to greatly change over the range of temperatures investigated. At ambient temperatures, SSP_{H_2O} of Cox was 132 and reduced to just 7 at 90°C. Therefore, a near two-order of magnitude reduction was seen in the effectiveness of self-sealing because of water flow. A reduction was also seen in the effectiveness of self-sealing because of active shear (SSP_r), although the reduction was not as marked as for water and the data showed considerable spread. The preliminary data for Callovo-Oxfordian claystone suggest that the favourable self-sealing properties of the rock reduce with temperature and become almost negligible at 90°C, that is in contradiction with what ULorraine and UGA found (Figure 9).

5 Modelling tools and approaches

5.1 Boom Clay

The hydro-mechanical behaviour of Boom Clay is reproduced with models such as the Drucker-Prager criterion (Drucker and Prager, 1952) or the Cam-Clay model. Many other constitutive mechanical laws have been developed to simulate the clay in various thermo-hydro-mechanical conditions. For example, the development of thermo-plastic strains by the increase of temperature was taken into account in models such as ACMEG-T (François, 2008) and in other thermo-mechanical cap models (Cui et al., 2000; Dizier, 2011). Dizier (2011) developed a thermo-mechanical model consisting in an extension of the cap model to thermo-plasticity. The model combines different plastic mechanisms, i.e., modified Cam-clay, friction angle criterion and a traction criterion. In addition to these three yield surfaces, a thermo-plastic mechanism is added based on the work done by Sultan (1997) and Cui et al. (2000). The thermo-plastic model is based on the model developed by Hueckel and Borsetto (1990) in which two plastic mechanisms were added to represent the thermo-mechanical behaviour of soils. These mechanisms make possible to reproduce the volume change induced by temperature and the decrease of the preconsolidation pressure with the increase of temperature. Figure 13 represents these mechanisms in the (p' , T) plane. The thermal yield limit (TY) reproduces the generation of volumetric thermal strain depending on the stress state or OCR of the clay. This curve is close to the p' axis because the soil is assumed to be

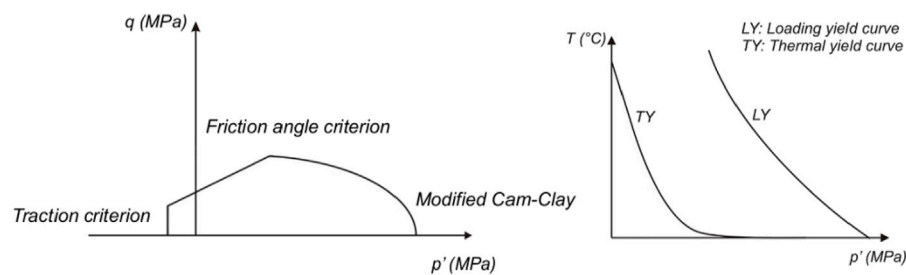


FIGURE 13
Thermal yield limit (TY) and loading yield limit (LY) in the (p', T) plane (Dizier, 2011; Charlier et al., 2010).

initially virgin of any temperature effects. The loading yield limit (LY) represents the decrease of the preconsolidation pressure with temperature.

Considering cross-anisotropic models with anisotropic properties of the clay helps to have a better understanding of the Boom Clay behaviour. The first integration of this elasto-plastic anisotropy was done during the TIMODAZ project (Charlier et al., 2010). Even if the simple approach proposed at that time already provided very promising results, anisotropic models for Boom Clay still need further investigations to completely describe its elasto-plastic response.

Some of the modelling exercises carried out using tests performed with Boom Clay (from triaxial tests to large-scale *in-situ* tests) and their main conclusions are summarised below. Some of these exercises were particularly useful for obtaining parameters.

- Within the framework of the EC project TIMODAZ, a backanalysis of several triaxial tests was performed (Dizier, 2011; TIMODAZ, 2010) to determine a set of mechanical parameters. The modelling results put in evidence that deviatoric behaviour is well represented when considering hardening or softening, but the volumetric behaviour is more difficult to capture. The main conclusion of these modelling activities is that a classical elasto-plastic model may be used to simulate qualitatively the deviatoric behaviour of the clay under drained and undrained conditions. The smooth transition between the elastic and plastic part may be captured thanks to well adapted hardening parameter values. In that way, the elastic domain is reduced and the plastic strains are generated earlier.
- A Drucker-Prager model, which takes into account the anisotropic nature of Boom Clay, was used to model a hollow cylinder test performed at EPFL during the TIMODAZ project (François et al., 2014). The anisotropy of the clay was considered by using a transverse elasticity and by an effective cohesion varying according to the angle between the stratification plane and the direction of the principal stress. This approach was implemented within the LAGAMINE finite element software (Collin, 2003). The comparison between observations and numerical results in the three directions confirmed the importance of the cross-anisotropy properties of the Boom Clay.
- The large scale PRACLAY Heater test (section 3.1) was modelled considering a Drucker-Prager model with a cross-

anisotropic elasticity and a hardening behaviour of the effective friction angle (Dizier et al., 2016; 2017). In this model, the temperature induces thermal elastic strains only and the thermo-plasticity was not considered. Distinct vertical and horizontal total stresses were imposed and a coefficient of earth pressure at rest (K_0) of 0.7 (based on Bernier et al., 2002; Bernier et al., 2007a; Dehandschutter et al., 2004; Cornet, 2009). The effective stresses were defined according to the Terzaghi's principle, the heat transfer using Fourier's law of conduction and the flow of water using the classic Darcy's law. The thermo-hydraulic properties selected were based on Bernier et al. (2007a), Bastiaens et al. (2006), Chen et al. (2011), Garitte et al. (2014), Horseman et al. (1987), Chen (2012), Chen et al. (2014). The mechanical properties of the excavation-damaged zone decreased due to the excavation and remained the same for the heating phase as their potential restoration requires a longer time (self-healing). Although the modelling results were in a good agreement with the observations, the following limitations were identified:

1. Blind predictions of Dizier (2011) showed that at this scale the effect of thermo-plasticity should be very limited in comparison with thermo-elastic models. The temperature around PRACLAY heater tests should induce only reversible deformations. This conclusion needs to be reconsidered with the current knowledge of the PRACLAY Heater test, which started in 2014.
2. In the modelling of the PRACLAY Heater test, the influence of the EDZ is limited to an abrupt variation of parameters with time. This description of the EDZ requires further investigations to improve the modelling of hydro-mechanical disturbances induced by the excavation (Chen et al., 2021; Chen et al., 2023 G.).
3. The viscous characteristics of Boom Clay were not taken into account while it is known that it exhibits a visco-elasto-plastic behaviour. This effect needs to be integrated in the constitutive models to simulate the long-term behaviour of the Boom Clay.

5.2 Callovo-Oxfordian claystone

In order to validate the rheological models at the scale of a HLW cell and, and if possible, to improve the determination of the parameters used, ANDRA set up from 2003 an *in situ* experimental programme to progressively:

- Confirm the thermal design parameters for the disposal
- Provide a better quantification for the THM processes around the HLW cells
- Perform some experiments to validate the concepts for the HLW cells

The *in-situ* tests in the MHM URL made it possible, through inverse analysis, to estimate certain THM parameters on a metric scale and to compare them with the measurements on samples (Garitte et al., 2014). For example, the inverse analysis of the thermal parameters (thermal conductivity, heat capacity) confirmed the low variability between the values obtained in the laboratory experiments and those measured in the field.

The small-scale thermal tests (TER, TED) demonstrated that the numerical simulations conducted with a linear thermo-poro-elastic model could accurately reproduce the temperature and the pore pressure variations, while also taking into consideration the thermal, mechanical and hydraulic anisotropy. From these tests, the sensitivity analyses showed that the major parameters were the stiffness of the Cox claystone, the permeability, and, to a lesser extent, the thermal conductivity and the Biot coefficient.

The first results from the full-scale HLW disposal cell demonstration test with the 2009 concept in the MHM URL (ALC1604) showed that the small-scale approach that was used, without considering the change in thermal parameters in the EDZ, enables a reasonable prediction of the temperature range. For the changes in the “far-field” pore pressure (several metres away from the heating cell), the influence of the modifications on the near-field hydro-mechanical properties caused by the cell excavation, remain low. However, in the near field, the purely linear poro-elastic approach is not good enough to correctly reproduce the change in pore pressure or the deformations. A more complete modelling approach is therefore required to better represent the physical processes in the fractured zone caused by cell excavation (variations in permeability, mechanical behaviour of fractured zone, etc.).

The analysis of the temperature, pressure and stress variations around the HLW cells as a function of the thermal load and of the inter-cell spacing was done internally using two well-known numerical simulation programs: Code-Aster and Code_Bright. UPC also performed the modelling on Code_Bright of the ALC1604 heating experiment (Tourchi et al., 2021).

In addition, some benchmarking exercises were carried out, for example:

- Constitutive model for the EDZ. A benchmark exercise was organised in 2012 to model the induced fracture networks around a drift (Seyedi et al., 2017; Guayacan, 2016). Several constitutive models were developed, divided into four main families: most were based on visco-elasto-plasticity, but damage-mechanics, rigid body spring and computational homogenised models were also tested. It was shown that accounting for material anisotropy and strain localisation treatment techniques could improve the results when elasto-visco-plastic models are used.
- THM modelling of the TED *in-situ* heating test. A benchmark exercise was organised as part of the DECOVALEX 2019 international program with the purpose to upscale the

THM modelling from small-size experiments (some cubic metres) to real-scale cell experiments (tens of cubic metres) and finally to the scale of the waste repository (cubic kilometres). It was based on the TED small-scale heating experiment (Conil et al., 2020) and focused on the THM behaviour of the undisturbed claystone in the far field (Seyedi et al., 2021). It was concluded that a good prediction of the evolution of temperature and pore pressure can be achieved if anisotropic poro-elastic behaviour is considered.

5.3 Opalinus Clay

The modelling of several large-scale heating experiments performed at the Mont Terri URL, such as the HE-E (Gaus et al., 2014) modelled by Garitte et al. (2017a) and the HE-D (Bossart et al., 2017), modelled by, e.g., Gens et al. (2007) and Garitte et al. (2017b), facilitated the hierarchical classification of cross-coupling between different THM processes in OPA:

- The strongest coupling was found from thermal to hydraulic and mechanical behaviour. Pore water pressure generation is mainly controlled by temperature increase, with thermal expansion being the primary contributor to strains and displacements.
- Significant but moderate effects result from the coupling of hydraulic to mechanical behavior. Dissipation of pore pressures induces additional displacements and strains, albeit smaller than thermally-induced deformations due to clay stiffness.
- Mechanical damage could theoretically impact hydraulic results, causing higher permeability, but the damaged zone’s size seems limited, with minimal impact.
- No noticeable coupling was observed from hydraulic to thermal behavior. Heat transport is predominantly by conduction, and material saturation remains constant during heating.
- Coupling from mechanical to thermal behavior is negligible. Subtle porosity variations in the clay host rock do not affect thermal conductivity, and mechanical energy dissipation is insignificant in the non-isothermal case of the HE-D experiment.

In the context of the FE experiment, various modelling exercises (e.g., Ewing and Senger, 2012; Senger, 2015; Garitte, et al., 2014; NAGRA, 2019) estimate key parameters, including temperature evolution, degree of saturation, pore water pressure, and strain in the Opalinus Clay. Scoping calculations using the THM code_Bright (Olivella et al., 1994; 1996), as reported in NAGRA (2019), yielded key conclusions:

- Peak temperatures at the heater surface range from approximately 100°C–195°C, depending on buffer properties.
- The maximum simulated temperature at the interface between buffer and rock in the direction of the bedding planes remains at 85°C, irrespective of buffer properties.
- Desaturation of the Opalinus Clay is limited.
- The combined effect of pore water flux and differential thermal expansion results in a maximum pore water pressure increase

of around 3 MPa at a distance between 7 and 15 m from the tunnel axis.

5.4 Modelling work done during HITEC

Numerical models taking into account multi-physical couplings in geometric configurations that may be complex (several materials, etc.) require sophisticated behaviour laws for which there is not always a simple way (e.g., analytical solutions) to validate the implementation. Benchmarks are then one of the ways to compare the different approaches with the international state of the art, to validate the results and to understand the differences between the models and their sensitivities. As mentioned before, several benchmark initiatives have previously been carried out, especially through the DECOVALEX (DEvelopment of COupled models and their VALidation against Experiments) project. This international research and model comparison collaboration was initiated in 1992 for advancing the understanding and modelling of THMC and chemical processes in geological systems. Over the last three phases of this project, the following *in situ* experiments involving claystones and high temperature have been modelled: the HE (D2015 Task B1) and FE experiments (D2023 Task C) in the Mont Terri URL and the TED, ALC1604 (D2019 Task E) and CRQ (D2023 Task A) experiments in the MHM URL. These benchmark exercises allowed to improve the interpretation of the *in situ* tests and led to scientific publications (some of which listed in the previous sections) that validate the modelling approaches and that can now be implemented to model and dimension different components of the storage facility and support the safety assessment.

The modelling of generic cases of a high-level waste repository was undertaken during HITEC to compare the output of the different codes and the behaviour of three clay host rocks (both in the near field and in the far field). The modelling of some of the laboratory experiments described in Section 4.2 was also carried out, and the last step of the benchmark consisted in modelling two full-scale *in-situ* heating experiments (described in Section 3). All this work is described in detail in de Lesquen et al. (2024).

A comparative 2D modelling exercise of the near and far field was carried out for three clay rocks considered to host radioactive waste repositories in Europe: the Boom Clay, the Callovo-Oxfordian claystone and the Opalinus Clay. The near-field generic case considered the problem of a single deposition drift during excavation, waiting and heating phases. Three subcases were considered: 1) isotropic elastic conditions, 2) anisotropic stress conditions with cross-anisotropic elasticity and thermo-elasticity and 3) anisotropic stress conditions with elasto-plasticity/damage. The goal of these subcases was to compare the numerical codes on fixed exercises (subcases 1 and 2) by prescribing the same boundary conditions and mechanical constitutive laws and properties, and to compare different approaches to reproduce the behaviour of the host rock and the development of the EDZ (subcase 3). Both unsupported and supported tunnels were considered. The far-field exercise considered the effect of heating further away from the disposal tunnels and over a much longer time period (1,000 years).

A brief description of the approaches of the various modelling teams and the main developments achieved during the project is given below:

- ANDRA ran the elastic cases on COMSOL Multiphysics and Code_Aster. In the framework of an ongoing scientific collaboration, Ineris developed a regularized anisotropic elastoplastic and damage model including both non-linear short- and long-term responses (Souley et al., 2024). This model was implemented in COMSOL Multiphysics and applied to subcase 3. The far-field model was also run on COMSOL Multiphysics.
- BGE worked with the numerical code FLAC3D and the open-source code OpenGeoSys. Within the latter, a material model for claystone, which incorporates its mechanical, thermal, and hydraulic behaviour, was developed and implemented (Mánica, 2018). The model falls within the frameworks of the elasto-viscoplasticity theory and the plasticity-creep partition approach (Chaboche, 2008), and it incorporates features relevant for the description of indurated clays behaviour: a non-linear yield criterion, strength and stiffness anisotropy, a non-associated flow rule, rate-dependency, strain hardening/softening, non-local regularisation, creep deformations, and permeability increase with damage. Concerning the thermal enhancement of the model, two main phenomena were considered for implementation (Tourchi et al., 2023): the continuous variation of mechanical properties (e.g., shear strength) with temperature, and the temperature-induced reversible expansive strains followed by, at some threshold temperature values, irreversible contractive strains.
- EDF used their in-house software Code_Aster and the LKR model based on Laigle (2004), Kleine (2007) and Raude (2015).
- EURIDICE/SCK•CEN used the finite element code COMSOL Multiphysics.
- LEI worked on the development of a constitutive model using the COMSOL Multiphysics. Thermo-poroelasticity was considered for the modelling of near field effects in the isotropic and anisotropic stress conditions. For modelling of the EDZ elastoplasticity was considered.
- The constitutive model of ULiege for the near field in the second subcase considered anisotropic elasticity, permeability, thermal conductivity, stress and Biot coefficient. They also developed a new THM second gradient model able to reproduce the strain localisation processes occurring within the EDZ (Song et al., 2023). The model to simulate the far field considered the anisotropy of the elasticity, the permeability, the thermal conductivity, the stresses and the Biot coefficient with two thermal loads (Rawat, 2023).
- UPC developed a fully coupled THM constitutive model for clay rocks for saturated and unsaturated states. The constitutive model is formulated within the framework of elastic-viscoplasticity, which considers non-linearity and softening after peak strength, anisotropy of stiffness and strength, as well as permeability variation due to damage. In addition, mechanical properties were coupled with thermal history (Song et al., 2024). The model was implemented in the finite element method software CODE_BRIGHT.

After fixing several discrepancies on the input parameters for the near-field generic cases, all teams obtained matching results for the isotropic elastic step. Some variations were however observed on the pressure and stress calculations in the anisotropic cases. Differences

in the THM formulations and assumptions made in the different codes may be the main reason for these disparities. The precise location of the integration point depending on the mesh and on the averaging method may also explain some discrepancies, especially at or near the contour of the tunnel where the gradients are the largest. The analysis of LEI showed that the water drainage condition on the tunnel boundary had no effect on the thermal state around the tunnel, but it had a significant impact on the hydro-mechanical response (Narkūnienė et al., 2022). The heating applied to the low-permeability claystone/poorly indurated clay results in pore pressure build-up because of the difference in the thermal expansion coefficients of water and of the solid matrix. As expected, the resulting overpressure is relatively low in the softer Boom Clay, but the exercise showed that the same heat load produced a very different pressure and stress responses in the Callovo-Oxfordian claystone and Opalinus Clay that have similar properties. All these elastic models predict some tensile effective horizontal stress at the borehole wall for the three clay host rocks. In reality, the excavation induces some fracturing in this area, and more advanced models are needed to account for the presence of the damaged zone. The last step of the near-field benchmark (modelling of the EDZ) gave an opportunity to improve the existing models and study the impact of heating on the extension of the EDZ (Song, 2023). The results of ULiège showed that the gap distance between the drift wall and the liner plays a significant role on the evolution of the strain localisation process. ANDRA's Comsol model was improved implementing a regularised anisotropic elastoplastic and damage model including both non-linear short and long-term response. The influence of damage and fracturing on the transport and viscous properties was also considered (Souley et al., 2024). This model was further developed to be able to take into account the decrease of strength with temperature that was observed in laboratory experiments (section 4.2.1). Different approaches were used but similar results were obtained, matching the EDZ geometry observed *in situ*. Some variations appear on the size of the damaged zone, but the high plastic strains are always localised in the very near field and all the models predict that heating for 10 years at constant power does not result in any EDZ expansion.

In the far-field benchmarking exercise, all teams considered an anisotropic poro-elastic behaviour—which is known to provide a good prediction of the evolution of both temperature and pore pressure (Seyedi et al., 2021)—and got matching results for the pressure and stress evolution at mid-distance between two parallel high-level waste cells. This outcome with six modelling teams and four different codes improves the confidence in these computations and the modelling approach used to dimension repositories. A sensitivity study performed by LaMcube on behalf of ANDRA with a phase-field model showed that when taking into account the presence of the EDZ, the extension of damage remains limited to the near field (Shao et al., 2024) and it has no impact on the pore pressure evolution in the far field.

The triaxial compression tests performed at different temperatures by ULorraine on heated Cox samples (section 4.2.1) were modelled by five teams. The BGE model developed by Mánica (2018) and implemented in the OpenGeoSys open-source code was applied successfully to this case. A non-local formulation was also employed by UPC in the simulation of these tests to allow a proper simulation of localisation phenomena. The constitutive model was

elasto-plastic and included softening and anisotropy of stiffness and strength and thermal effects. Realistic drainage boundary conditions were adopted. The family of yield surfaces were based on a hyperbolic approximation to the Mohr-Coulomb envelope. A parametric study was performed to check the influence of the rate of temperature rise and of the resting period. The agreement with experimental results was satisfactory (Song et al., 2024). This exercise showed that a good understanding of the boundary conditions is essential for a correct interpretation of the experiments and use of their results. The modelling of the heating phase under undrained conditions revealed the generation of overpressures when fast heating rates were applied, that may induce some damage in the samples. It may explain the strength reduction observed in the tests conducted at low confining pressures, implying that the heating phase was not conducted under fully drained conditions. *Postmortem* analysis of samples heated in the ALC1604 and CRQ *in situ* heating experiments actually showed no changes in the mechanical properties. Some of the models were nevertheless developed to take into account the observed strength reduction with temperature (Souley et al., 2024) and its impact on the near-field and far-field calculations will be evaluated.

Five teams modelled the ALC1605 *in-situ* heating experiment (Section 3.2) in 2D (LEI and ULg) and in 3D (Andra, BGE and EDF). After the initial predictive modelling step, using the Callovo-Oxfordian parameters provided in the first benchmarking exercises, large differences were observed between the modelling and the measurements. Most teams underestimated the anisotropic impact of the cell excavation on the pore pressure. On the other hand, plane strain conditions do not allow longitudinal fluid flow and heat flux; as a result, the temperature and pore pressure evolution on heating was overestimated when 2D models were used. In the interpretative modelling step, the teams had access to the historical data and could adapt their models to match the results and improve the understanding of the behaviour of the Callovo-Oxfordian claystone. To this aim the models were modified by reducing the value of the applied heat flow, modifying the Cox material properties, considering the heat loss, or introducing an EDZ. However, none of this resulted in a significant improvement of the match between predictions and measurements. More advanced models are needed to take into account the processes occurring around the tunnels (e.g., modification of hydraulic properties within the EDZ, creep).

Four teams modelled the large-scale *in situ* PRACLAY Heater test (Section 3.1): BGE, ULiège, UPC and EURIDICE/SCK CEN. The benchmark exercise started by an academic case, using an elastic model with parameters appropriate for Boom Clay, and then increased in complexity. The results of the first step showed a good agreement between the involved teams when modelling the experiment with elastic and elasto-plastic constitutive laws. In all cases, the anisotropy of the clay was taken into account, with anisotropic intrinsic permeability and thermal conductivity, and the elastic behaviour was modelled with cross-elasticity. For the second phase, ULiège used an isotropic strain hardening Drucker-Prager elastoplastic model. An EDZ with a higher permeability was introduced and the parameters of the sound layer were optimised in order to get a good agreement with the *in-situ* measurements. They also introduced a strain-dependent isotropic evolution of the hydraulic permeability tensor and the shear strain reproducing the stiffness degradation curve. To model the PRACLAY experiment UPC used the advanced Hyperbolic Mohr-Coulomb model with hardening-

softening and nonlocal formulation, with the air gap approach to represent the contact between the host clay and the concrete lining. A satisfactory agreement with field observations was achieved by both teams, and the analyses showed that pore pressures depend strongly on stiffness parameters and that thermal pressurization is larger when the drained bulk modulus increases. This modelling work also showed that intrinsic permeability plays a significant role in the liquid dissipation and, therefore, changing the intrinsic permeability can significantly modify the pore pressure evolution.

An overall conclusion of these modelling exercises is that very consistent results can be obtained with different codes using a poro-elastic approach when the parameters and boundary conditions are correctly set. As this type of model is known to predict correctly the temperature and pressure evolutions in the far field, this benchmark increases the confidence and shows the robustness of the modelling approach used to design the repositories. More advanced models are however needed to account for the processes occurring around the tunnels (e.g., modification and strain dependency of hydraulic and mechanical properties within the EDZ, creep). The modelling of laboratory experiments showed the importance of a good understanding of the test setups and of the boundary conditions and helped explain some of the results.

6 Summary and conclusions

This paper summarised the knowledge about the thermo-hydro-mechanical behaviour of three clay rocks with potential to host radioactive waste repositories in Europe: the Boom Clay, the Callovo-Oxfordian claystone and the Opalinus Clay. Experimental and modelling activities carried out in the framework of the EURAD-HITEC project concerning these materials have also been synthesised. The focus has been placed on the impact of elevated temperature on these properties.

Working at high temperature with claystones poses experimental challenges, and in this sense experimental improvements were achieved during the HITEC project. Different testing cells (triaxial, oedometric and shear ring) and monitoring tools (X-ray and neutron tomography) were used by the different partners and adapted to work at high temperature, although most tests were performed below 90°C. The use of triaxial cells with heating collars, though not uncommon, has been particularly developed during the project and tests at temperatures as high as 150°C were performed by ULorraine, although with considerable evaporation of the samples. Adding heating to the direct shear rig of BGS was particularly complicated. X-ray CT and neutron tomographic images were used to follow the evolution of cracks, but a need to improve the quality of images and the testing protocols (recreate *in situ* stress conditions and measure the hydraulic conductivity of the interface during self-sealing) was identified.

The impact of the testing protocols on the results obtained is always a concern. For example, it cannot be ruled out that thermal loading rates applied, much higher than those to be expected in a repository, could damage the samples and consequently their subsequent behaviour. Furthermore, the particular stress conditions during the tests may affect the results. Thus, the formation of microcracks in Cox claystone induced by the thermal expansion of the pore water under uniaxial conditions—leading to a significant decrease in the peak strength with temperature—may be reduced by application of confining pressure

during heating. In fact, the modelling of the triaxial tests revealed the generation of overpressures when fast heating rates were applied under undrained conditions. This overpressure could induce some damage in the samples that may explain the strength reduction observed in the triaxial tests conducted at low confining pressures, which in turn would imply that the heating phase of these tests was not conducted under fully drained conditions. Also in relation to the stress conditions, while K_0 experiments allow the measurement of formation overpressures, they impose a slightly artificial boundary condition under which the sealing of indurated materials such as OPA and Cox may be more difficult. This geometry may also limit some failure mechanisms.

Important hydro-mechanical couplings between peak pore water pressure, temperature, permeability and confining stress were identified. Temperature was seen to have a clear effect on the fracture shear properties of both Cox and Opalinus claystones (increase in peak strength, residual strength and shear modulus). The triaxial compression tests showed that temperature may have a negative impact on the short-term strength to failure of the Cox claystone. But if this THM damage were induced, it would probably be limited to the very near field of the EDZ, where the confining pressure is the lowest. At 100°C and 150°C, the peak strength and the stiffness of the Cox claystone increased, irrespective of the sample orientation, because the pore water evaporated and the samples got desaturated. The thermal pressurisation tests on Opalinus Clay and Callovo-Oxfordian claystone samples did not show any strong impact of heating on the clay permeability.

Many parameters could influence the efficiency of the self-sealing process: the calcium carbonate content, the sample orientation with respect to bedding, the opening of the initial artificial crack, and the temperature. The tests performed confirmed the self-sealing capacity of the Cox claystone, even when heated at 90°C. Provided that the clay content of the samples was high enough, self-sealing was an efficient mechanism whatever the experimental conditions. Temperature may have a slight delaying effect on the self-sealing process though. However, the effectiveness of self-sealing processes as a result of hydration and shear was seen to reduce significantly at elevated temperatures. Indeed, fracture roughness, which likely plays a role in this process, is reduced by the presence of water during the re-shear phase and by temperature.

The results of the laboratory experiments confirmed that the claystone keeps its good mechanical and self-sealing properties, even when heated at high temperature (up to 100°C). Nonetheless, considering the heat output of the waste and the thermally induced pore water pressures, a repository should be located at a depth below which thermally induced pore water pressures could remain lower than the *in-situ* stress. Overall, confidence was gained in the positive impact of the self-sealing process on the restoration of the initial sealing properties of the clay host rock, especially because the duration of the laboratory experiments was much shorter than the repository time scale.

The modelling activities undertaken during HITEC intended to compare the output of the different codes used by the participants and the behaviour of the three clay host rocks. The benchmarks comprised the modelling of near-field and far-field generic cases of a high-level waste repository, two large-scale *in situ* heating experiments and triaxial laboratory tests performed in the framework of the project.

The near-field generic case showed the pore pressure build-up resulting from the heating applied to the clay host rock, and, as expected, a relatively lower overpressure in the softer Boom Clay than in the Opalinus clay and the Cox claystone. All the models predicted that the high plastic strains (associated to the EDZ development) are always localised in the very near field. Heating for 10 years at constant power would not result in any EDZ expansion. In the far-field model, six modelling teams using four different codes got matching results for the pressure and stress evolution at mid-distance between two parallel high-level waste cells, which improves confidence in the modelling approach used to dimension repositories.

The modelling of laboratory experiments showed the importance of a good understanding of the test setups and of the boundary conditions and helped explain some of the results. Modelling of the heating phase under undrained conditions revealed the generation of overpressures when fast heating rates were applied, inducing some damage in the samples. This may explain the strength reduction observed in the tests conducted at low confining pressures, implying that the heating phase was not conducted under fully drained conditions.

When modelling the ALC1605 *in situ* heating experiment in 2D and 3D, the teams successfully managed to reproduce the anisotropic response of the clay host rocks to excavation and heating, but most teams underestimated the pore pressure response induced by the cell excavation. The use of 2D models does not allow longitudinal fluid flow and heat flux; hence, they also overestimate the temperature and pore pressure evolution on heating. The evolutions of temperature and pore pressure were well modelled in the far field with an anisotropic poro-elastic approach, but more advanced models are needed to account for the processes occurring around the tunnels (e.g., modification of hydraulic and mechanical properties within the EDZ, creep). Better results were obtained when modelling the large-scale *in situ* experiment PRACLAY Heater test, because a strain-dependent isotropic evolution of the hydraulic permeability tensor and the shear strain reproducing the stiffness degradation curve. The parameters that played a significant role to match the *in situ* measurements were the stiffness of the sound clay rock and of the damaged clay, and the permeabilities in both zones.

An overall conclusion of these modelling exercises is that very consistent results can be obtained with different codes using a poro-elastic approach when the parameters and boundary conditions are correctly set. As this type of model is known to predict correctly the temperature and pressure evolutions in the far field, this benchmark increases the confidence and shows the robustness of the modelling approach used to design the repositories. More advanced models are however needed to account for the processes occurring around tunnels (e.g., modification and strain dependency of hydraulic and mechanical properties within the EDZ, creep). Finally, this project gave an opportunity to improve some of the codes and to validate some recent developments.

Author contributions

MV: Conceptualization, Writing–original draft, Writing–review and editing. PB: Data curation, Investigation, Software,

Writing–original draft. FC: Data curation, Investigation, Software, Writing–original draft. RC: Data curation, Investigation, Writing–original draft. CL: Investigation, Software, Writing–original draft, Writing–review and editing, Conceptualization. AD: Data curation, Investigation, Writing–original draft, Writing–review and editing, Conceptualization. GE: Investigation, Software, Writing–original draft. AG: Investigation, Software, Writing–original draft. CG: Data curation, Investigation, Writing–original draft. DG: Data curation, Investigation, Writing–original draft, Writing–review and editing, Conceptualization. JH: Data curation, Investigation, Writing–original draft. CI: Data curation, Investigation, Writing–original draft. OL: Supervision, Writing–original draft, Conceptualization. SL: Writing–original draft. AN: Investigation, Writing–original draft, Software. ES: Investigation, Software, Writing–original draft. A-BT: Writing–original draft.

Funding

The author(s) declare that financial support was received for the research, authorship, and/or publication of this article. European Union's Horizon 2020 Research and Innovation Programme under grant agreement No. 847593.

Acknowledgments



Conflict of interest

The authors declare that the research was conducted in the absence of any commercial or financial relationships that could be construed as a potential conflict of interest.

Publisher's note

All claims expressed in this article are solely those of the authors and do not necessarily represent those of their affiliated organizations, or those of the publisher, the editors and the reviewers. Any product that may be evaluated in this article, or claim that may be made by its manufacturer, is not guaranteed or endorsed by the publisher.

Supplementary material

The Supplementary Material for this article can be found online at: <https://www.frontiersin.org/articles/10.3389/fnuen.2025.1436490/full#supplementary-material>

References

- Agboli, M., Grgic, D., Moumni, M., and Giraud, A. (2024). Study under X-ray tomography of the impact of self-sealing process on the permeability of the Callovo-Oxfordian claystone. *Rock Mech. Rock Eng.* 57 (6), 4213–4229. doi:10.1007/s00603-023-03350-y
- Alcolea, A., Marschall, P., and FE Team (2019). FE-Modelling Task Force/Task 1: validation of thermally induced THM effects in the rock around the FE-tunnel. *NAGRA Arbeitsbericht NAB*, 19–040.
- Armand, G., Bumbieler, F., Conil, N., de La Vaissière, R., Bosgiraud, J. M., and Vu, M. N. (2017). Main outcomes from *in situ* thermo-hydro-mechanical experiments programme to demonstrate feasibility of radioactive high-level waste disposal in the Callovo-Oxfordian claystone. *Eng* 9, 415–427. doi:10.1016/j.jrmge.2017.03.004
- Auvray, C., Grgic, D., Morlot, C., Fourreau, E., and Talandier, J. (2015). “X-ray tomography applied to self-healing experiments on argillites. 13th ISRM international congress of rock mechanics, montréal.” Québec, Canada.
- Awarkeh, M. (2023). Investigation of the long-term behaviour of Boom clay. (PhD thesis). École Natl. des Ponts Chaussées.
- Baldi, G., Borsetto, M., and Hueckel, T. (1987). *Calibration of mathematical models for simulation of thermal, seepage and mechanical behaviour of Boom Clay*. Luxembourg: Commission of the European Communities. Nuclear science and Technology EUR 10924.
- Baldi, G., Hueckel, T., Peano, A., and Pellegrini, R. (1991). “Nuclear science and technology EUR 13365/2,” in *Developments in modelling of thermo-hydro-mechanical behaviour of Boom Clay and clay-based buffer (vol.2)*. Luxembourg: Commission of the European Communities.
- Bastiaens, W., Bernier, F., and Li, X. L. (2006). *An overview of long-term HM measurements around HADES URF*. In: *EUROCK 2006 Multiphysics coupling and long term behaviour in rock mechanics*, 15–26.
- Belmokhtar, M., Delage, P., Ghabezloo, S., and Conil, N. (2017). Thermal volume changes and creep in the callovo-oxfordian claystone. *Springer Verl.* 50 (9), 2297–2309. doi:10.1007/s00603-017-1238-7
- Bernier, F., Li, X. L., and Bastiaens, W. (2007a). Twenty-five years’ geotechnical observation and testing in the Tertiary Boom clay formation. *Géotechnique* 57 (2), 229–237. doi:10.1680/geot.2007.57.2.229
- Bernier, F., Li, X. L., Bastiaens, W., Ortiz, L., Van Geet, M., Wouters, L., et al. (2007b). *SELFRAC: Fractures and self-healing within the excavation disturbed zone in clays*. Final report, European Commission, CORDIS website, EUR 22585, 56. Available at: <https://cordis.europa.eu/project/id/FIKW-CT-2001-00182/reporting>
- Bernier, F., Li, X. L., Verstricht, J., Barnichon, J. D., Labiouse, V., Bastiaens, W., et al. (2002). *Clipeux. Report eur 20619*. Luxembourg: Commission of the European Communities.
- Bossart, P., Jaeggi, D., and Nussbaum, C. (2017). Experiments on thermo-hydro-mechanical behaviour of Opalinus clay at Mont Terri rock laboratory, Switzerland. *J. Rock Mech. and Geotechnical Eng.* 9 (3), 502–510. doi:10.1016/j.jrmge.2016.11.014
- Bossart, P., and Thury, M. (2008). *Mont Terri rock laboratory. Project, programme 1996 to 2007 and results. Rep. Swiss geol. Surv. 3, swisstopo, 3084 wabern, Switzerland*.
- Braun, P. (2019). *Thermo-hydro-mechanical behaviour of the Callovo-Oxfordian claystone Effects of stress paths and temperature changes*. PhD Thesis. Université Paris-Est.
- Bumbieler, F., Plúa, C., Tourchi, S., Vu, M. N., Vaunat, J., Gens, A., et al. (2021). Feasibility of constructing a full-scale radioactive high-level waste disposal cell and characterization of its thermo-hydro-mechanical behavior. *Int. J. Rock Mech. Min. Sci.* 137, 104555. doi:10.1016/j.ijrmms.2020.104555
- Bumbieler, F., Plúa, C., Vu, M. N., and Armand, G. (2024). Assessment of a full-scale *in situ* heater experiment based on the French high-level waste disposal cell concept conducted in the Callovo-Oxfordian claystone. *Tunn. Undergr. Space Technol.* 153, 106004. doi:10.1016/j.tust.2024.106004
- Buyens, M., and Put, M. (1984). *Heat transfer experiment in Boom clay. 9th European conference on thermophysical properties. 17–21 september*. Manchester, UK.
- Chaboche, J. L. (2008). A review of some plasticity and viscoplasticity constitutive theories. *Int. J. Plasticity* 24 (10), 1642–1693. doi:10.1016/j.ijplas.2008.03.009
- Charlier, R., Chalandar, S., Collin, F., and Dizier, A. (2010). *Deliverable D13 – annex 4. In situ heating test ATLAS in Mol. TIMODAZ project, F16W-CT-2007-036449*. Available online at: https://igdtp.eu/wp-content/uploads/2018/08/TIMODAZ-13_D13mainreportv5.pdf.
- Chen, G., Li, X., Dizier, A., Verstricht, J., Sillen, X., and Levasseur, S. (2023a). Characterization of Boom Clay anisotropic THM behaviour based on two heating tests at different scales in the HADES URL. *Geol. Soc.* 536 (1), 51–74. doi:10.1144/sp536-2022-72
- Chen, G. J. (2012). *Modeling of PRACLAY tests: improved HM parameters of Boom Clay based on in-situ measured PWP around PG, SAC 41 meeting*. Internal presentation.
- Chen, G. J., Dizier, A., Li, X. L., Verstricht, J., Sillen, X., and Levasseur, S. (2021). Numerical prediction of the large-scale *in situ* PRACLAY heater test in the Boom clay. *Rock Mech. Rock Eng.* 54, 2197–2218. doi:10.1007/s00603-021-02405-2
- Chen, G. J., Li, X. L., Sillen, X., and Levasseur, S. (2023b). Determination of the anisotropic thermal conductivity of the Boom Clay based on a combined numerical interpretation of two *in situ* heater tests at different scales. *Acta Geotech.* 18, 127–147. doi:10.1007/s11440-022-01555-z
- Chen, G. J., Maes, T., Vandervoort, F., Sillen, X., Van Marcke, P., Honny, M., et al. (2014). Thermal impact on damaged Boom clay and Opalinus clay: permeameter and isotatic tests with μ CT scanning. *Rocks Mech. Rock Eng.* 47 (1), 87–99. doi:10.1007/s00603-012-0334-y
- Chen, G. J., Sillen, X., Verstricht, J., and Li, X. L. (2011). ATLAS III *in situ* heating test in Boom clay: field data, observation and interpretation. *Comput. Geotechnics* 38 (5), 683–696. doi:10.1016/j.compgeo.2011.04.001
- Chen, W. Z., Gong, Z., Ma, Y. S., Yu, H. D., and Li, X. L. (2017). *Temperature effect on the drained creep behavior of Boom clay. Clay conference, davos, 2017*.
- Coll, C., Collin, F., Radu, J. P., Illing, P., Schroeder, C. H., and Charlier, R. (2006). The report of long term behaviour of Boom clay – influence of clay viscosity on the far field pore pressure distributions. *Internal report, Université of Liège, Liège, 154 pp*.
- Coll, C. (2005). “Endommagement des roches argileuses et perméabilité induite au voisinage d’ouvrages souterrains,” in *Thèse de doctorat* (Grenoble 1: Université Joseph Fourier).
- Collin, F. (2003). *Couplages thermo-hydro-mécaniques dans les sols et les roches tendres partiellement saturés*. Thèse de doctorat. Université de Liège, Faculté des Sciences Appliquées.
- Conil, N., Vitel, M., Plúa, C., Vu, M. N., Seyedi, D., and Armand, G. (2020). *Situ investigation of the THM behavior of the callovo-oxfordian claystone. Rock. Mech. Rock. Eng.* 53, 2747–2769. doi:10.1007/s00603-020-02073-8
- Cornet, F. H. (2009). *In situ stress measurement campaign at SCK-CEN Underground Laboratory. École et Observatoire des Sciences de la Terre, Université de Strasbourg, Internal report*.
- Croisé, J., Mayer, G., Marschall, P., Matray, J. M., Tanaka, T., and Vogel, P. (2006). Gas threshold pressure test performed at the Mont Terri Rock Laboratory (Switzerland): experimental data and data analysis. *Oil and Gas Sci. Technol.* 61 (5), 631–645. doi:10.2516/ogst:2006003
- Cui, Y. J., Le, T. T., Tang, A. M., Delage, P., and Li, X. L. (2009). Investigating the time-dependent behaviour of Boom clay under thermomechanical loading. *Géotechnique* 59 (4), 319–329. doi:10.1680/geot.2009.59.4.319
- Cui, Y. J., Sultan, N., and Delage, P. (2000). A thermomechanical model for saturated clays. *Can. Geotechnical J.* 37, 607–620. doi:10.1139/t99-111
- Cuss, R. J., Harrington, J. F., Sathar, S., Norris, S., and Talandier, J. (2017). The role of the stress-path and importance of stress history on the flow of water along fractures and faults; an experimental study conducted on kaolinite gouge and Callovo-Oxfordian mudstone. *Appl. Clay Sci.* 150, 282–292. doi:10.1016/j.clay.2017.09.029
- Cuss, R. J., Milodowski, A., and Harrington, J. F. (2011). Fracture transmissivity as a function of normal and shear stress: first results in Opalinus clay. *Phys. Chem. Earth* 36, 1960–1971. doi:10.1016/j.pce.2011.07.080
- Cuss, R. J., Milodowski, A. E., Harrington, J. F., and Noy, D. J. (2009). *Fracture transmissivity test of an idealised fracture in Opalinus clay. British geological survey commissioned report, CR/09/163*. Nottingham, 74.
- Cuss, R. J., Sathar, S., and Harrington, J. F. (2012). *Fracture transmissivity test in Opalinus clay; test conducted on a realistic fracture. British geological survey commissioned report, CR/12/132*. Nottingham, 63.
- Dao, L. Q. (2015). “Etude du comportement anisotrope de l’Argile de Boom. PhD thesis, CERMES, Ecole Nationale des Ponts et Chaussées.” Paris.
- De Beer, A., Carpentier, R., Manfroy, P., and Heremans, R. (1977). Preliminary studies of an underground facility for nuclear waste burial in a tertiary clay formation. *Rockstore Conf.* 3, 771–780. doi:10.1016/b978-1-4832-8406-4.50129-9
- De Bruyn, D., and Labat, S. (2002). The second phase of ATLAS: the continuation of a running THM test in the HADES underground research facility. *Mol. Eng. Geol.* 64(2–3), 309–316. doi:10.1016/S0013-7952(01)00109-0
- De Bruyn, D., and Labat, S. (2002). The second phase of ATLAS: the continuation of a running THM test in the HADES underground research facility. *Mol. Eng. Geol.* 64 (2–3), 309–316. doi:10.1016/S0013-7952(01)00109-0
- Dehandschutter, B., Vanduycke, S., Sintubin, M., Vandenberghe, N., Gaviglio, P., Sizun, J. P., et al. (2004). Microfabric of fractured Boom Clay at depth: a case study of brittle-ductile transitional clay behaviour. *Appl. Clay Sci.* 26, 389–401. doi:10.1016/j.clay.2003.12.013
- Delage, P., Cui, Y. J., and Tang, A. M. (2010). Clays in radioactive waste disposal. *J. Rock Mech. Geotechnical Eng.* 2 (2), 111–123. doi:10.3724/sp.j.1235.2010.00111
- Delage, P., Sultan, N., and Cui, Y. J. (2000). On the thermal consolidation of Boom Clay. *Can. Geotechnical J.* 37, 343–354. doi:10.1139/t99-105

- De La Vaissière, R., Armand, G., and Talandier, J. (2015). Gas and water flow in an excavation-induced fracture network around an underground drift: a case study for a radioactive waste repository in clay rock. *J. Hydrology* 521, 141–156. doi:10.1016/j.jhydrol.2014.11.067
- De Lesquen, C., Vu, M. N., Plua, C., Simo, E., Tatmir, A., León, P., et al. (2024). Modelling report on the effect of temperature on clay host rocks behaviour. Final version as of 06/06/2024 of deliverable 7.6 of the HORIZON 2020 project EURAD. *EC Grant Agreem. N. 847593*, 288. Available at: <https://www.ejp-eurad.eu/publications/eurad-d76-hitec-modelling-report-effect-temperature-clay-host-rocks-behaviour>
- Deng, Y. F., Cui, Y. J., Tang, A. M., Li, X. L., and Sillen, X. (2012). An experimental study on the secondary deformation of Boom Clay. *Appl. Clay Sci.* 59 (60), 19–25. doi:10.1016/j.clay.2012.02.001
- Dizier, A. (2011). *Caractérisation des effets de température dans la zone endommagée autour des tunnels de stockage de déchets nucléaires dans des roches argileuses*. PhD thesis. Université de Liège.
- Dizier, A., Chen, G. J., and Li, X. L. (2018). *State of the art: thermo-hydro-mechanical behavior of the Boom Clay*. Internal report. Mol: Euridice.
- Dizier, A., Chen, G. J., Li, X. L., Leysen, J., Verstricht, J., Troullinos, I., et al. (2016). *The start-up phase of the PRACLAY heater test*. EURPH16_025. Mol, Belgium.
- Dizier, A., Chen, G. J., Li, X. L., and Rypens, J. (2017). *The PRACLAY Heater test after two years of the stationary phase*. EURPH17_043. Mol, Belgium.
- Dizier, A., Chen, G. J., Verstricht, J., Li, X. L., Sillen, X., and Levasseur, S. (2021). The large-scale *in situ* PRACLAY heater test: first observations on the *in situ* thermo-hydro-mechanical behaviour of Boom clay. *Int. J. Rock Mech. Min. Sci.* 137, 104558. doi:10.1016/j.ijrmm.2020.104558
- Djéran, I. (1991). *Etude des diffusions thermique et hydraulique dans une argile soumise à un champ de température*. (Thèse de Doctorat). École nationale des ponts et chaussées, Marne-la-Vallée, France.
- Drucker, D. C., and Prager, W. (1952). Soil mechanics and plastic analysis or limit design. *Q. Appl. Math.* 10 (2), 157–165. doi:10.1090/qam/48291
- Ewing, J., and Senger, R. (2012). *Evolution of temperature, pressure and saturation in the bentonite buffer: scoping calculations in support of the design of the full-scale emplacement experiment at the Mont Terri URL*. Unpubl. NAGRA interner bericht NIB 10–040.
- Ferrari, A., Favero, V., Manca, D., and Laloui, L. (2013). Geotechnical characterization of core samples from the geothermal well Schlattigen SLA-1. NAGRA Arbeitsbericht NAB. NAB, 12–50. Wettingen, 69. Available at: <https://nagra.ch/downloads/arbeitsbericht-nab-12-50/>
- François, B. (2008). *Thermo-plasticity of soils at various saturation state: application to nuclear waste disposal*. PhD thesis. École Polytechnique Fédérale de Lausanne.
- François, B., Labiouse, V., Dizier, A., Marinelli, F., Charlier, R., and Collin, F. (2014). Hollow cylinder tests on Boom clay: modelling of strain localization in the anisotropic excavation damaged zone. *Rock Mech. Rock Eng.* 47 (1), 71–86. doi:10.1007/s00603-012-0348-5
- Garitte, B., Gens, A., Vaunat, J., and Armand, G. (2014). Thermal conductivity of argillaceous rocks: determination methodology using *in situ* heating tests. *Rock Mech. Rock Eng.* 47 (1), 111–129. doi:10.1007/s00603-012-0335-x
- Garitte, B., Nguyen, T. S., Barnichon, J. D., Graupner, B. J., Lee, C., Maekawa, K., et al. (2017a). Modelling the Mont Terri HE-D experiment for the Thermal-Hydraulic-Mechanical response of a bedded argillaceous formation to heating. *Environ. Earth Sci.* 76, 345–420. doi:10.1007/s12665-017-6662-1
- Garitte, B., Shao, H., Wang, X. R., Nguyen, T. S., Li, Z., Rutqvist, J., et al. (2017b). Evaluation of the predictive capability of coupled thermo-hydro-mechanical models for a heated bentonite/clay system (HE-E) in the Mont Terri Rock Laboratory. *Environ. Earth Sci.* 76, 64–18. doi:10.1007/s12665-016-6367-x
- Gaus, I., Garitte, B., Senger, R., Gens, A., Vasconcelos, R., Garcia-Sineriz, J. L., et al. (2014). *The HE-E experiment: lay-out, interpretation and THM modelling combining d2.2-11. Final report on the HE-E experiment and d3.2-2: modelling and interpretation of the HE-E experiment of the PEBS project*. NAGRA working report NAB 14-53, wettingen, Switzerland and EU PEBS project report downloadable from. Available online at: <http://www.pebs-eu.de/>
- Gbewade, C. A. F., Grgic, D., Giraud, A., and Schoumacker, L. (2024). Experimental study of the effect of temperature on the mechanical properties of the Callovo-Oxfordian claystone. *Rock Mech. Rock Eng.* 106, 4191–4212. doi:10.1007/s00603-023-03630-7
- Gens, A., Vaunat, J., Garitte, B., and Wileveau, Y. (2007). *In-situ* behaviour of a stiff layered clay subject to thermal loading. Observations and interpretation. *Géotechnique* 57 (2), 207–228. doi:10.1680/geot.2007.57.2.207
- Giot, R., Auvray, C., and Talandier, J. (2019). Self-sealing of claystone under X-ray nanotomography. *Geol. Soc.* 482 (1), 213–223. doi:10.1144/SP482.4
- Grgic, D., Bésuelle, P., and Cuss, R. (2023b). Technical report on thermal effects on near field properties. Final version as of 01.11.2023 of deliverable D7.3 of the HORIZON 2020 project EURAD. *EC Grant Agreem. no 847593*. Available at: <https://www.ejp-eurad.eu/publications/eurad-d73-technical-report-thermal-effects-near-field-properties>
- Grgic, D., Imbert, C., Harrington, J., and Tamayo-Mas, E. (2023a). Technical report on thermal effects on far field properties. Final version as of 01.11.2023 of deliverable D7.5 of the HORIZON 2020 project EURAD. *EC Grant Agreem. no 847593*. Available at: <https://www.ejp-eurad.eu/publications/d75-final-technical-report-effect-temperature-far-field-properties>
- Guayacan Carrillo, L. M. (2016). *Analysis of long-term closure in drifts excavated in Callovo-Oxfordian claystone: roles of anisotropy and hydromechanical couplings*. (PhD thesis). Université Paris-Est.
- Gunzburger, Y., and Cornet, F. H. (2007). Rheological characterization of a sedimentary formation from a stress profile inversion. *Geophys. J. Int.* 168 (1), 402–418. doi:10.1111/j.1365-246X.2006.03140.x
- Hoek, E., and Brown, E. T. (1980). Empirical strength criterion for rock masses. *J. Eng. Div.* 106 (9), 1013–1035. doi:10.1061/ajgeb6.0001029
- Horseman, S. T., Winter, M. G., and Entwistle, D. C. (1987). *Geotechnical characterization of Boom clay in relation to disposal of radioactive waste*. Publications of the European Communities, EUR 1087 EN. Luxembourg.
- Hueckel, T., and Borsetto, M. (1990). Thermoplasticity of saturated clays: experimental constitutive study. *J. Geotechnical Eng.* 116 (12), 1765–1777. doi:10.1061/(asce)0733-9410(1990)116:12(1765)
- Hueckel, T., François, B., and Laloui, L. (2009). Explaining thermal failure in saturated clays. *Géotechnique* 53 (3), 197–212. doi:10.1680/geot.2009.59.3.197
- Jahn, S., Mrugalla, S., and Stark, L. (2016). *Endlagerstandortmodell SÜD - Teil II: Zusammenstellung von Gesteinseigenschaften für den Langzeitsicherheitsnachweis, Bundesanstalt für Geowissenschaften und Rohstoffe (BGR)*. Hannover.
- Jobmann, M., Breustedt, M., Li, S., Polster, M., and Schirmer, S. (2013). *Investigations on THM effects in buffer, EDZ and argillaceous host rock*. Final Report. TEC-09-2012-AB, DBE TECHNOLOGY, Peine.
- Kleine, A. (2007). *Modélisation Numérique du Comportement des Ouvrages Souterrains par une Approche Viscoplastique*. PhD thesis.
- Labiouse, V., Sauthier, C., and You, S. (2014). Hollow cylinder simulation experiments of galleries in Boom Clay Formation. *Rock Mech. Rock Eng.* 47 (1), 43–55. doi:10.1007/s00603-012-0332-0
- Laigle, F. (2004). *Modèle Conceptuel pour le Développement de Lois de Comportement adaptées à la Conception des Ouvrages Souterrains*. PhD thesis.
- Le, T.-T. (2011). 2008. Comportement thermo-hydro-mécanique de l'argile de Boom. (PhD thesis). CERMES, Ecole Nationale des Ponts et Chaussées. Paris, France.
- Li, X. L., Dizier, A., Chen, G. J., Verstricht, J., and Levasseur, S. (2023). “Forty years of investigation into the thermo-hydro-mechanical behaviour of Boom Clay in the HADES URL,” 536. London: Geological Society, 33–49. doi:10.1144/sp536-2022-103
- Lima, A. (2011). *Thermo-hydro-mechanical behaviour of two deep Belgium clay formations: Boom Clay and Ypresian clays*. PhD Thesis. Universitat Politècnica de Catalunya, Spain.
- Mair, R., Taylor, R., and Clarke, B. (1992). *Repository tunnel construction in deep clay formations*. Luxembourg: Commission of the European Communities. Nuclear science and Technology EUR 13964.
- Mánica, M. A. (2018). *Analysis of underground excavations in argillaceous hard soils - weak rocks*. PhD thesis. Barcelona: Technical University of Catalonia, 196. Available online at: <http://hdl.handle.net/10803/663452>.
- Marschall, P., Horseman, S., and Gimmi, T. (2005). Characterisation of gas transport properties of the Opalinus clay, a potential host rock formation for radioactive waste disposal. *Oil and Gas Sci. Technol.* 60 (1), 121–139. doi:10.2516/ogst:2005008
- Mertens, J., Bastiaens, W., and Dehandschutter, B. (2004). Characterisation of induced discontinuities in the Boom Clay around the underground excavations (URF, Mol, Belgium). *Appl. Clay Sci.* 26, 413–428. doi:10.1016/j.clay.2003.12.017
- Mohajerani, M., Delage, P., Sulem, J., Monfared, M., Tang, A. M., and Gatmiri, B. (2012). A laboratory investigation of thermally induced pore pressures in the Callovo-Oxfordian claystone. *Int. J. Rock Mech. Min. Sci.* 52, 112–121. doi:10.1016/j.ijrmm.2012.02.012
- Monfared, M. (2011). *Couplages température-endommagement-perméabilité dans les sols et les roches argileuses*. PhD thesis. École Nationale des Ponts et Chaussées.
- NAGRA (2002a). Demonstration of disposal feasibility for spent fuel, vitrified high-level waste and long-lived intermediate-level waste (Entsorgungsnachweis). *NAGRA Tech. Rep. NTB*, 02–05. Available at: <https://nagra.ch/en/downloads/technical-report-ntb-02-23-2/>
- NAGRA (2002b). Synthèse der geowissenschaftlichen Untersuchungsergebnisse - Entsorgungsnachweis für abgebrannte Brennelemente, verglaste hochaktive sowie langlebige mitteltaktive Abfälle. *NAGRA Tech. Ber. NTB*, 02–03. Available at: <https://nagra.ch/downloads/technischer-bericht-ntb-02-03/>
- NAGRA (2014). *SGT Etappe 2: Vorschlag weiter zu untersuchender geologischer Standortgebiete mit zugehörigen Standortarealen für die Oberflächenanlage: Geologische Grundlagen Dossier VI Barriereigenschaften der Wirt- und Rahmgesteine*. Nagra Technischer Bericht. NTB 14–02 Dossier VI. Available at: <https://nagra.ch/en/downloads/technical-report-ntb-15-02-2/>

- NAGRA (2019). Technical Report NTB 15-02. Implementation of the full-scale emplacement experiment at Mont Terri: design, construction and preliminary results. Available online at: <https://nagra.ch/en/downloads/technical-report-ntb-15-02-2/>
- Narkūnienė, A., Poskas, G., Justinavicius, D., and Kilda, R. (2022). THM response in the near field of an HLW disposal tunnel in the callovo-oxfordian clay host rock caused by the imposed heat flux at different water drainage conditions. *Minerals* 12, 1187. doi:10.3390/min12101187
- Nguyen, X. P., Cui, Y. J., Tang, A. M., Deng, Y. F., Li, X. L., and Wouters, L. (2013). Effects of pore water chemical composition on the hydro-mechanical behavior of natural stiff clays. *Eng. Geol.* 166, 52–64. doi:10.1016/j.enggeo.2013.08.009
- Olivella, S., Gens, A., Carrera, J., and Alonso, E. E. (1994). Nonisothermal multiphase flow of brine and gas through saline media. *Transp. Porous Media* 15, 271–293. doi:10.1007/bf00613282
- Olivella, S., Gens, A., Carrera, J., and Alonso, E. E. (1996). Numerical formulation for a simulator (CODE_BRIGHT) for the coupled analysis of saline media. *Eng. Comput.* 13 (7), 87–112. doi:10.1108/02644409610151575
- ONDRAF/NIRAS (2013). *Research, Development and Demonstration (RD&D) plan for the geological disposal of high level and/or long-lived radioactive waste including irradiated fuel if considered as waste. State-of-the-art report as of December 2012.* Belgian Agency for Radioactive Waste for Enriched Fissile Materials. NIRONDR-TR 2013-12 E.
- Péguyon, F. (2021). *Modélisations physique et numérique de la zone endommagée autour de galeries creusées dans l'argile de Boom.* (PhD thesis). University of Lorraine.
- Pellet, F. (2007). *Expertise sur le comportement différé des argilites.* Rapport interne ANDRA N° CRP0FLO070024.
- Plúa, C., Vu, M. N., Armand, G., Ouraga, Z., Yu, Z., Shao, J. F., et al. (2024). Numerical investigation of the thermal hydrofracturing behavior of the Callovo-Oxfordian claystone. *Geomechanics Energy Environ.* 40, 100596. doi:10.1016/j.gete.2024.100596
- Plúa, C., Vu, M. N., de La Vaissière, R., and Armand, G. (2023). *In situ* thermal hydrofracturing behavior of the callovo-oxfordian claystone within the context of the deep geological disposal of radioactive waste in France. *Rock Mech. Rock Eng.* 57, 4265–4283. doi:10.1007/s00603-023-03618-3
- Poller, A., Mayer, G., and Croisé, J. (2007). Two-phase flow analysis of gas tests in Opalinus clay core specimen: complementary analysis. *Mont. Terri TN*, 2007–2101.
- Raude, S. (2015). *Prise en compte des sollicitations thermiques sur les comportements instantané et différé des géomatériaux.* PhD thesis, Université de Lorraine Géoresources.
- Rawat, A. (2023). *EURAD HITEC Technical Report Task 2.3: influence of temperature on clay-based material behaviour-far field generic case.*
- Rebours, H., Andre, G., Cruchaudet, M., Dewonck, S., Distinguin, M., Drouiller, Y., et al. (2005). *Callovo-Oxfordien - Rapport de synthèse.* D.RP.ADPE.04.1110, Andra. Paris: France.
- Robinet, J. C., Sardini, P., Coelho, D., Parneix, J.-C., Prêt, D., Sammartino, S., et al. (2012). *Effects of mineral distribution at mesoscopic scale on solute diffusion in a clay-rich rock. Example of the Callovo-Oxfordian mudstone of Bure (France).* *Water Resources Research* 48: W05554.
- Romero, E., and Gómez, R. (2013). *Water and air permeability tests on deep core samples from Schlattigen SLA-1 borehole.* NAGRA Arb. Ber. NAB 13–51. Wettingen, Switzerland: NAGRA.
- Senger, R. (2015). *Scoping calculations in support of the design of the full-scale emplacement experiment at the Mont Terri URL, evaluation of the effects and gas transport phenomena.* Wettingen, Switzerland: Nagra Work Report NAB, 13–98.
- Seyedi, D. M., Armand, G., and Noiret, A. (2017). “Transverse Action” – a model benchmark exercise for numerical analysis of the Callovo-Oxfordian claystone hydromechanical response to excavation operations. *Comput. Geotechnics* 85, 287–305. doi:10.1016/j.compgeo.2016.08.008
- Seyedi, D. M., Plúa, C., Vitel, M., Armand, G., Rutqvist, J., Birkholzer, J., et al. (2021). Upscaling THM modeling from small-scale to full-scale *in-situ* experiments in the Callovo-Oxfordian claystone. *Int. J. Rock Mech. Min. Sci.* 144, 104582. doi:10.1016/j.ijrmm.2020.104582
- Shao, J.-F., Yu, Z., Liu, Z., Vu, M.-N., and Armand, G. (2024). Numerical analysis of thermo-hydromechanical process related to deep geological radioactive repository. *Deep Resour. Eng.* 1, 100001–109305. doi:10.1016/j.deepr.2024.100001
- Song, F., Gens, A., Collico, S., and Grgic, D. (2024). *Fully coupled THM constitutive model for clay rocks: formulation and application to laboratory tests.* UNSAT-WASTE 2023. Shanghai, China.
- Song, H., Cormann, G., and Collin, F. (2023). Thermal impact on the excavation damage zone around a supported drift using the 2nd gradient model. *Rock Mech. Rock Eng.* 56 (10), 7575–7598. doi:10.1007/s00603-023-03440-x
- Souley, M., de Lesquen, C., Vu, M.-N., and Armand, G. (2024). *Effect of temperature on the short and long term THM behaviour of Callovo-Oxfordian claystone - implications for a radioactive waste repository.* 4th international conference on coupled processes in fractured geological media: observation, modeling, and application (CouFrac2024). Kyoto: Japan.
- Stavropoulou, E., Andò, E., Roubin, E., Lenoir, N., Tengattini, A., Briffaut, M., et al. (2020). Dynamics of water absorption in callovo-oxfordian claystone revealed with multimodal X-ray and neutron tomography. *Front. Earth Sci.* 8, 6. doi:10.3389/feart.2020.00006
- Sultan, N. (1997). *Etude du comportement thermo-mécanique de l'Argile de Boom: Expériences et modélisation.* (PhD thesis). École Natl. des Ponts Chaussées.
- Tang, A. M., Cui, Y. J., and Barnel, N. (2008). Thermo-mechanical behaviour of a compacted swelling clay. *Géotechnique* 58 (1), 45–54. doi:10.1680/geot.2008.58.1.45
- Terzaghi, K., Peck, R., and Mesri, G. (1996). *Soil mechanics in engineering practice.*
- Tourchi, S., Mánica, M. A., Gens, A., Vaunat, J., Vu, M. N., and Armand, G. (2023). *A thermomechanical model for argillaceous hard soils-weak rocks: application to THM simulation of deep excavations in claystone.* *Géotechnique*. doi:10.1680/jgeot.23.00023
- Tourchi, S., Vaunat, J., and Gens, A. (2019). *THM modelling of the ALC1604 experiment.* *Rapport Andra n°CGRPCMFS190016.*
- Tourchi, S., Vaunat, J., Gens, A., Bumbieler, F., Vu, M.-N., and Armand, G. (2021). A full-scale *in situ* heating test in Callovo-Oxfordian claystone: observations, analysis and interpretation. *Comput. Geotechnics* 133, 104045. doi:10.1016/j.compgeo.2021.104045
- Vandenbergh, N., De Craen, M., and Wouters, L. (2014). The Boom Clay geology, from sedimentation to present-day occurrence, a review. Royal Belgian institute of natural sciences. *Memoirs Geol. Surv. Belg.*, 60–2014. Available at: https://gsb.naturalsciences.be/wp-content/uploads/2024/09/Memoirs_60_Vandenbergh_advertisement.pdf
- Van Geet, M., Bastiaens, W., and Ortiz, L. (2008). Self-sealing capacity of argillaceous rocks: review of laboratory results obtained from the SELFRAC project. *Phys. Chem. Earth, Parts A/B/C* 33 (Suppl. 1), S396–S406. doi:10.1016/j.pce.2008.10.063
- Van Geet, M., Lalieux, P., Van Humbeeck, H., Dierckx, A., De Preter, P., Gens, R., et al. (2007). *PRACLAY success criteria.* NIRONDR note 2007-1144 (internal report).
- Van Marcke, P., Li, X. L., Bastiaens, W., Verstricht, J., Chen, G. J., Leysen, J., et al. (2013). *The design and installation of the PRACLAY In-Situ Experiment.* EURIDICE Report. Mol, Belgium, 13–129.
- Wang, L., Bornert, M., and Chanchole, S. (2013). Micro-scale experimental investigation of deformation and damage of argillaceous rocks under hydric and mechanical loads. *Poromechanics V*, 1635–1643. doi:10.1061/9780784412992.193
- Wileveau, Y. (2005). THM behaviour of host rock (HE-D) experiment: progress report. Part 1, Technical Report TR 2005-03. Mont Terri Project.
- Wileveau, Y., Cornet, F., Desroches, J., and Blumling, P. (2007a). Complete *in situ* stress determination in an argillite sedimentary formation. *Phys. Chem. Earth Parts A/B/C* 32 (8–14), 866–878. doi:10.1016/j.pce.2006.03.018
- Wileveau, Y., and Rothfuchs, T. (2007). THM behaviour of host rock (HE-D) Experiment: Study of Thermal effects on Opalinus Clay. *Mont Terri Tech. Rep.*, 2006–2101.
- Wileveau, Y., Su, K., and Ghoreychi, M. (2007b). A heating experiment in the argillites in the meuse/haute-marne underground research laboratory. In: 11th international conference on environmental remediation and radioactive waste management. Bruges, 939–944. doi:10.1115/ICEM2007-7276
- Yu, L., Rogiers, B., Gedeon, M., Marivoet, J., De Craen, M., and Mallants, D. (2013). A critical review of laboratory and *in-situ* hydraulic conductivity measurements for the Boom Clay in Belgium. *Appl. Clay Sci.* 75–76, 1–12. doi:10.1016/j.clay.2013.02.018
- Yu, L., Weetjens, E., Vietor, T., and Hart, J. (2010). TIMODAZ (Contract Number: FI6W-CT-2007-036449). Integration of TIMODAZ results within the safety case and recommendations for repository design (D14). *Final Rep. WP6*, 48.
- Yuan, H., Agostini, F., Duan, Z., Skoczylas, F., and Talandier, J. (2017). Measurement of Biot's coefficient for Cox argillite using gas pressure technique. *Int. J. Rock Mech. Min. Sci.* 92, 72–80. doi:10.1016/j.ijrmm.2016.12.016
- Zhang, C. L., Armand, G., and Conil, N. (2015). Investigation on the anisotropic mechanical behavior of the Callovo-Oxfordian clay rock. Final Report. *GRS* 360.
- Zhang, C. L., Czaikowski, O., and Rothfuchs, T. (2010). Thermo-Hydro-Mechanical behaviour of the Callovo-Oxfordian clay rock. *GRS – 266*, 2010. Available at: <https://www.grs.de/sites/default/files/publications/GRS-266.pdf>
- Zhang, C. L., Rothfuchs, T., Jockwer, N., Wiczorek, K., Dittrich, J., Müller, J., et al. (2007). Thermal effects on the Opalinus clay. A joint heating experiment of ANDRA and GRS at the Mont Terri URL (HE-D project). Final report. *Mont Terri Proj. Tech. Rep. TR 2007-02 GRS Rep.* 224. Available at: https://www.grs.de/sites/default/files/publications/grs-224_0.pdf
- Zhang, F., Xie, S. Y., and Shao, J. F. (2012). *Groupement de Laboratoires-Géomécanique, Fiche GM6: Effets de la température sur le comportement des argilites. Etude expérimentale et modélisations des effets de la température sur le comportement des argilites.* Rapport Andra n° C.RP.0LML.11.0004.